

UNCLASSIFIED//~~FOR OFFICIAL USE ONLY~~



Defense Intelligence Reference Document

Acquisition Threat Support

8 March 2010

ICOD: 1 December 2009

DIA-08-1001-006

Space Access: Where We've Been . . . and Where We Could Go

UNCLASSIFIED//~~FOR OFFICIAL USE ONLY~~

This document is made available through the declassification efforts
and research of John Greenewald, Jr., creator of:

The Black Vault



The Black Vault is the largest online Freedom of Information Act (FOIA) document clearinghouse in the world. The research efforts here are responsible for the declassification of hundreds of thousands of pages released by the U.S. Government & Military.

Discover the Truth at: <http://www.theblackvault.com>

Space Access: Where We've Been . . . and Where We Could Go

Prepared by:

(b)(3):10 USC 424

Defense Intelligence Agency

Author:

(b)(6)

Administrative Note

COPYRIGHT WARNING: Further dissemination of the photographs in this publication is not authorized.

This product is one in a series of advanced technology reports produced in FY 2009 under the Defense Intelligence Agency, (b)(3):10 USC 424 Advanced Aerospace Weapon System Applications (AAWSA) Program. Comments or questions pertaining to this document should be addressed to (b)(3):10 USC 424;(b)(6), AAWSA Program Manager, Defense Intelligence Agency, ATTN: (b)(3):10 USC 424 Bldg 6000, Washington, DC 20340-5100.

Contents

Introduction.....	v
Propulsion Perspective.....	1
Hypersonic Configuration Concepts.....	2
Thermodynamics and Materials.....	16
The Qu Tube.....	23
Rocket Propulsion.....	25
Up-and-Down Operations.....	30
Launch Options.....	33
Atmospheric Variations.....	35
Conclusion.....	37
Appendix A: Historical Perspective.....	43
Appendix B: Aeropropulsion Integrated Vehicle.....	46
Appendix C: TAV Operational Costs.....	47
Appendix D: Landing Ellipses for Hypersonic Gliders.....	48

Figures

Figure 1. Hardware Flow.....	vi
Figure 2. Impact of Air-Breathing Rocket.....	1
Figure 3. HSVS Hypersonic Cruise Aircraft Showing True Skin Temperature.....	3
Figure 4. Hypersonic Rocket-Powered Glider Hypersonic Air-Breathing Cruiser.....	4
Figure 5. Delta-Lifting Body Designs.....	5
Figure 6. Martin Marietta X-24 A & B Research Gliders.....	7
Figure 7. Detailed Design Analyses Show the Weight Trends are as Much a Function of Configuration Family as Lift-to-Drag Ratio.....	9
Figure 8. High-Performance Hypersonic Glide Aircraft.....	10
Figure 9. NASA Langley Wing-Body Configuration WB-004 with Critical Areas for Wing Bodies Identified.....	11
Figure 10. FDL-7C/D and FDL-7MC Lifting-Body Configuration.....	12
Figure 11. FDL-7C/D with a DuPont Retractable Inward-Turning Inlet.....	12
Figure 12. Comparison of FDL-7C/D and Model 176.....	13
Figure 13. Sufficient Cross Range (L/D) Means There is No Waiting to Return.....	14
Figure 14. Hypersonic Glider Characteristics.....	15
Figure 15. Both Delta Planform Lifting Body (Dynasoar) and Model 176 Offer Superior Landing Performance.....	16
Figure 16. McDonnell Aircraft Company Roll-Bonded Titanium Structure.....	17

Figure 17. Model 176 in the McDonnell Douglas Hypervelocity Impulse Tunnel18
Figure 18. FDL-7C/D, Model 176 Entry Temperature Distribution19
Figure 19. Even At Mach 12, Embedded Vortices in the Boundary Layer Alter the
Local Heat Transfer19
Figure 20. Thermographic Phosphor Image of Model 176 at Near-Maximum
Angle of Attack.....20
Figure 21. From L/D Maximum to Maximum Angle of Attack, There Is Always a
Cool Sub-layer Adjacent to the Wall20
Figure 22. This 1988 SEP Bordeaux SiC/SiC Panel Could Sustain Temperatures of
up to 3,000°F.....21
Figure 23. UBE Corporation's Tyranno Cloth.....21
Figure 24. A Porous Nickel Tip Oozing Water21
Figure 25. FDL ASSET Flight-Tested From Orbital Speeds to Evaluate 1960s
Materials22
Figure 26. Heat Pipe Shuttle Leading Edge Designed and Built by McDonnell
Douglas Astronautics22
Figure 27. Boost-Glide Strategic Vehicle with Pratt & Whitney XLR-129 Rocket
Engine Installed25
Figure 28. XLR-12925
Figure 29. Two Rocket Air-Breathing Rocket Cycles to Mach 5.527
Figure 30. HOTOL Evolution: From Aerodynamic Optimum Configuration to
Practical Launcher Configuration27
Figure 31. LACE Air-Breathing Rocket29
Figure 32. The FDL-7 Class of Vehicles29
Figure 33. Takeoff and Landing Speeds of Minimum-Sized Launchers.....30
Figure 34. Horizontal launch Not Practical Unless Weight Ratio Less Than Four ...31
Figure 35. Propellant Tanks That Are Not Reentry Vehicles Greatly Reduce
System Weight33
Figure 36. Simple Horizontal Integration and Vertical Launch Provides Rapid
Launch Capability34
Figure 37. A Vertical Launch Complex Provides Vertical Toss Back Booster
Recovery and Horizontal Landing Facilities for the Hypersonic Gliders 34
Figure 38. A 1964 MDC Astronautics, St. Louis, Briefing.....35
Figure 39. Earth's Atmosphere36
Figure 40. FDL-5 Scale Model of A Stage and One-Half.....37
Figure 41. The FDL-7 and Model 176 Class of Hypersonic Gliders.....37
Figure 42. Hypersonic Decelerating.....38
Figure 43. Where We Are Today39
Figure 44. Where We Could Be If We Can Recapture the Engineering Confidence
and Expertise of the Apollo/Saturn V Era40
Figure 45. TAV Operational Costs47
Figure 46. Landing Ellipse.....48

Tables

Table 1. Characteristics of Selected Flight Dynamics Laboratory Hypersonic
Glider Configurations During the 1958-68 Timeframe6
Table 2. Elements of the Space Infrastructure Shown in Figure 4441

Space Access: Where We've Been . . . and Where We Could Go

Introduction

Development of commercial access to space by our budding space-faring civilization is a straightforward effort dominated by propulsion and reliability. The initial focus should be on schedulable, dependable access to and from low Earth orbit (LEO). For years we have known the means to accomplish such a task but have lacked a dedicated organized effort. The key requirement is to develop a robust and not necessarily a low-cost infrastructure, without which commercial exploitation of LEO and the moon will not be possible. This is a matter of skill; operational hardware based on durable, reliable, and demonstrated components; and operational systems. It is not necessarily a matter of technology. However, technology discovery and development are necessary for future space travel beyond Earth's environs. This paper addresses these issues by providing a running account of the historical details associated with the development of the myriad systems proposed and tested to provide access to space.

Among the many advances in space access that will be possible in the future,¹ the key technology developments will be in the area of propulsion, because without these we are confined to our solar system by flight times limited to a project team's functional life. The Pioneer spacecraft were fortunate to be monitored for 20 years. However, the issue facing our spaceflight organizations is the lack of a durable, consistent, schedulable, and frequent hardware system to and from space assets such as the International Space Station.

In October 1958, the author's job in the vertical wind tunnel at Wright-Patterson Air Force Base abruptly changed; hypersonic and high-temperature flows became a new focus. What was then the Aircraft Laboratory was to become the Air Force Flight Dynamics Laboratory (AFFDL), with a focus on space flight. Al Draper of the AFFDL began working with a select group of aerospace firms on hypersonic gliders. The initial requirement from the Air Force was to quickly find operational access to space. Technology application, hardware design and fabrication with an innovative application, and extending the industrial capabilities of the time were very much the issue, as exemplified by the Lockheed A-12/SR-71. When asked about space access at the time, a group of Aerospace Corporation

responsibility for space access, that Air Force's focus switched to surveillance, communication, and Global Positioning System satellites.

In the late 1950s, there existed a predisposition—forced by the military competition between the United States and the former Soviet Union—to use rockets derived from military ballistic missiles. That decision curtailed efforts to develop alternatives to chemical rockets together with practical commercial developments. With the orbiting of Sputnik, the aircraft path to space, as represented by the X series of planes, ended with the X-15. With the X-15's demise, all efforts to fly aircraft to space ended, replaced by the more familiar (but less practical) strategy of loudly blasting to space with expendable rockets derived from undertested ballistic missile hardware, as documented in early failures.

Like their ballistic missile progenitors, current expendable rockets can be launched only once. With the exception of the experimental Delta Clipper developed and operated by William Gaubatz and the late Pete Conrad, no operational launcher has ever successfully aborted. In this context, a reusable launcher is simply an expendable with some parts reused a few times. Thus, neither the United States nor the Soviet Union/Russia has ever realized a truly commercial approach to space travel, although the Soviets came close to taking the first step with the since-terminated Energia/Buran system. Both the United States and the Soviet Union/Russia historically have generated a large number of concepts that could fly directly to space and return on a sustained, frequent, scheduled basis. An all-up air breather such as the NASP was to solve that problem and fly directly to space and return. Developing an operational mach 12 to 14 aircraft with air-breathing propulsion presents a serious design, engineering, and fabrication challenge analogous to the SR-71 Blackbird.

Propulsion Perspective

In exiting Earth's atmosphere, the propulsion system and configuration are inexorably linked. A hypersonic glider exits the atmosphere on either a rocket booster or a first stage of a two-stage-to-orbit aircraft. As such, it usually exits the atmosphere quickly, and the key exit design considerations are the high transonic aerodynamic and the mechanical loads encountered in the exit trajectory. Whether for a new rocket launcher or the U.S. space shuttle, the phenomenon is the same: the peak mechanical loads occur during exit. In this case, the exit aerodynamics are important but not vital. The vital aerodynamics and thermodynamics (aerothermodynamics) are in the entry glide, where thermal loads are maximal and must be controlled. The vehicle must always be controlled in flight so its attitude and direction are within limits set by the aerothermodynamics. The angle-of-attack limits are very close for high-performance hypersonic gliders, as their glide angle of attack is 11 to 15 degrees, not the 45 degrees of the space shuttle. Even the Russian Buran had a lower glide angle of attack than the shuttle; a TsAGI report given to the author by Vladimir Neyland shows it to have been about 30 to 35 degrees.² Like the Buran, the high-performance glider is best controlled by an automatic integrated flight control system that monitors the thermodynamic state of the vehicle, as well as its aerodynamic and trajectory states. The sensor array provides real-time information to the control system that can maintain the correct attitude in a manner a human controller could not accomplish. So it is this phase of the flight that designs the hypersonic glider.

The exception is when powered by an air-breathing rocket (HOTOL, Skylon, and LACE), which must remain lower in the atmosphere until reaching the air-breathing rocket transition to conventional rocket. The configuration for the air-breathing rocket is different, as it must have a retractable air inlet in the mach 0 to 5 range but does not determine the vehicle configuration. The impact is significant, as the carried oxidizer is reduced in the heaviest initial portion of the flight, as shown in Figure 2 for a Delta Clipper-type design with an aerospike nozzle tested by Konstantin Feotkiskov. The example is from a Senior Capstone Design Study Team from Parks College, Saint Louis University, circa 1992, and is based on the engineering reports the author was permitted to read from the library of Konstantin Feotkiskov, an aerospace designer and cosmonaut. The question, as always, is, why bother with air-breathing systems at all if they are that much of a challenge? The answer is to consider a partial air-breathing system based on available hydrogen/oxygen rockets that operate to about mach 5.5. It operates in a flight region where the carried oxidizer quantities are the greatest. An operational system is sought that is capable of a large number of flights per year. The fewer resources required for launch, the greater ease with which the system can operate and the greater potential to operate from more bases.

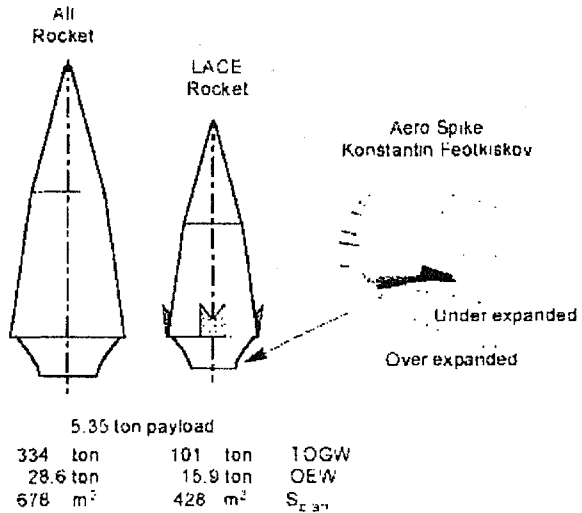


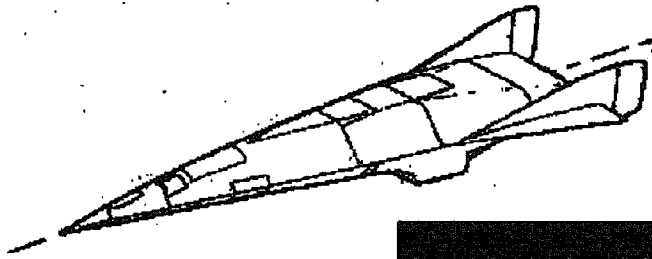
Figure 2. Impact of Air-Breathing Rocket

The Russian design bureaus are to thank for arriving at a concept that eliminated the noisy and hazardous air-breather takeoff and for increasing the operational flexibility of the British HOTOL concept. Glebe Lozino-Lozinski had a concept for a spacecraft with a 7-metric-ton payload carried atop an Antonov An-225, with a second An-225 carrying the liquid hydrogen and launch facilities and staff.³ The An-225 was in fact a mobile launch facility; it could literally launch a satellite for any facility that could accommodate a B-747 or an MDC-11. With Rolls Royce or General Electric engines, the An-225 becomes a more easily maintained vehicle with better altitude performance.

The An-225's empennage is modified from the An-124's single vertical and horizontal empennage to an 'H' configuration. This permits the powered hypersonic glider to easily lift off the top of the vehicle, as the MBB Sanger wind tunnel test demonstrated. Most commercial transport aircraft larger than ERJ 170 are potential mobile launch platforms for space tourism, point-to-point cargo, or orbital facilities support. Most of the commercial passenger equipment can be removed, with just enough equipment remaining for a launch crew. The fuselage is strengthened and fitted with external mountings for the hypersonic glider. The landing gear need not be modified, as the same maximum weight as the commercial transport will be maintained. The flight control system would be adapted to automatically maintain the correct launch trajectory until separation. A second modified transport would be modified to carry the liquid hydrogen and liquid air to fuel the hypersonic vehicle, along with maintenance and support crew. The intent is to use the automatic launch checkout the author witnessed at Baikanour in 1988, wherein a Soyuz that arrived on its train carrier at 0500 hours launched carrying a Progress capsule at 1715 hours the same day. That should make a local launch possible within hours of arriving at the specified airport launch departure site. These two elements can provide a commercial space launch facility that requires no special or dedicated operational base.

Hypersonic Configuration Concepts

The configuration and the propulsion system are linked through aerothermopropulsion integration. This approach is not new, as a wide spectrum of configurations and concepts existed in the 1960s. One such McDonnell Aircraft Company concept is shown in Figure 3. This potential operational mach 12 cruise vehicle was developed for the U.S. government as a strike reconnaissance vehicle taking off from a U.S. Air Force base. The concept was to provide on-demand reconnaissance in force operations. However, as was the case with all such efforts in the 1960s, none of the aircraft derived from the "flight-to-space" efforts reached a hardware stage. Individuals working on these projects were convinced that the industrial capability existed to design and fabricate these vehicles, and that such vehicles were technically feasible. The concepts varied widely among different nations, but all had as their goal a transportation system to space that had commercial potential. This discussion is provided to discriminate between rocket-powered hypersonic gliders and hypersonic cruisers with an air-breathing propulsion system.



McDonnell Aircraft
Advanced Design Dept.
1958 to 1967
Mr. H. D. Altis, Director

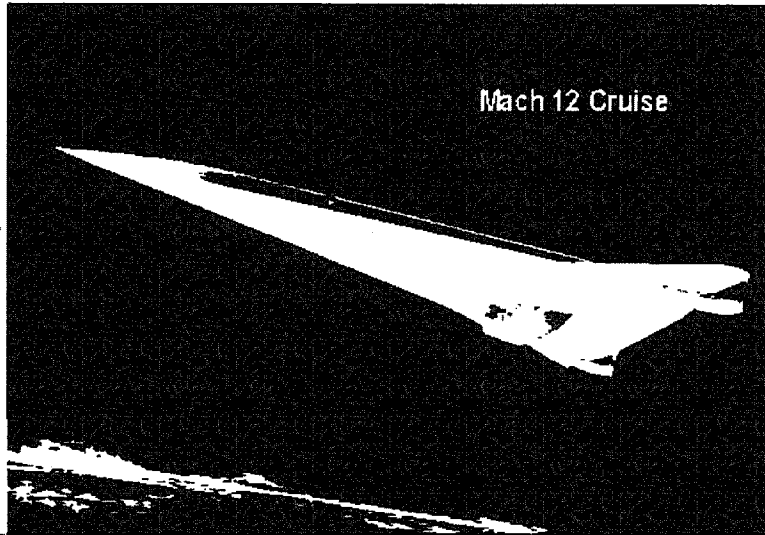


Figure 3. HSVS Hypersonic Cruise Aircraft Showing True Skin Temperature

A wide variety of configurations for recoverable spacecraft are possible. But if the requirements for a transportation system capable of traveling to and returning from space are to be met, the configurations spectrum is significantly narrowed. Two basic configuration types emerge. One configuration is for a hypersonic glider powered by either rocket or air-breathing rocket cycle propulsion that can operate as air-breathing propulsion to mach 5.5 or less. A versatile variable-capture, inward-turning inlet⁴ can be integrated with the vehicle configuration derived from the FDL series of hypersonic gliders developed by the U.S. Air Force Flight Dynamics Laboratory (AFFDL)⁵ and the work of the McDonnell Douglas Astronautics Company. Because of the mass ratio to orbit, these configurations are vertical takeoff and horizontal landing vehicles, exemplified by the upper-left vehicle in Figure 4. This vehicle is usually an upper stage in a two-stage-to-orbit rather than a single-stage-to-orbit vehicle.

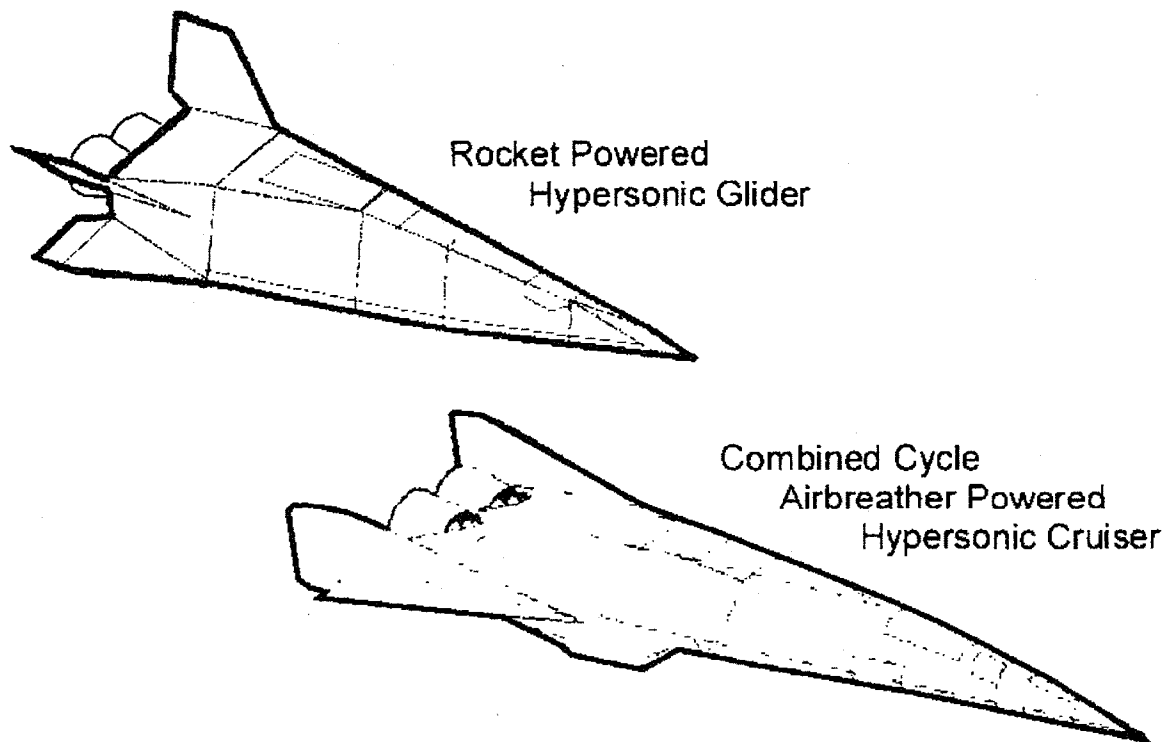


Figure 4. Hypersonic Rocket-Powered Glider and Hypersonic Air-Breathing Cruiser

The second configuration is for air-breathing propulsion systems operating at between mach 6 and mach 14 that require a propulsion-configured vehicle, where the underside of the vehicle is an integral part of the propulsion system (forming most of the air-capturing inlet). This is typified by the lower-right vehicle in Figure 4. The thermally integrated, air-breathing, combined-cycle configuration concept is derived from the McDonnell Douglas (St. Louis) Advanced Design organization. The vehicle concept initially conceived in the late 1950s and early 1960s was an air-breathing propulsion-configured vehicle accelerated by a main rocket in the aft end of the body, as shown in Figure 3. The vehicle's underside is the propulsion system; the engine is in the engine module.

Both basic shapes are functions of τ —that is, for a given planform area, the cross-sectional distribution is determined by the volume required. τ was reported in D. Küchemann's book on supersonic aerodynamics⁶ as:

$$\tau = \frac{V_{\text{total}}}{S_{\text{plan}}^{1.5}} \quad (1)$$

The only configuration discussed in the book in any detail is the rocket-powered hypersonic glider. The hypersonic glider has greater near-term potential to become an operational system, considering the failure of the National Aerospace Plane (NASP) to reach a functional hardware stage.

Whatever goes into orbit must enter the atmosphere many times if it is to be a sustained-use vehicle. If it is to be a commercial vehicle, then the flexibility to land wherever the commercial customers are is essential. Consider how successful FedEx, UPS, or DHL would be if there were only two pickup and delivery sites in the United States and a few more elsewhere in the world. A ballistic capsule has even fewer landing options, and a saltwater landing and recovery is too costly to be commercially feasible. What is needed is a hypersonic glider with the flexibility to enter when necessary, without waiting, and to land at different operational bases, just as a transport might. There were three serious competitors in the United States with respect to hypersonic glider configurations: the AFFDL at Wright-Patterson Air Force Base, the McDonnell Douglas Corporation (MDC), and the Lockheed Corporation.

NASA Ames and NASA Langley were also generating hypersonic configurations, but NASA's views on hypersonic gliders (fundamentally research and development projects) and their glide range requirements differed from those of the three organizations listed above. That difference is clearly exemplified by the difference between the operational requirements of an experimental aircraft (such as X-1, X-2, X-10, X-15, or X-20) that flies infrequently and at the convenience of the research organization and those of an operational Air Force or Navy aircraft that must be able to fly on any day in almost any weather when needed (also a Russian spacecraft operational rule). From the middle of the 1960s to the early 1970s, the U.S. Air Force and NASA had disagreements over the operational capability of these aircraft and their requirements. As a result, each went its own development direction, and much of the originality and practicality of the AFFDL concepts has not been reflected in the space access configurations developed by NASA. There was a final attempt to apply the AFFDL's philosophy of a high lift-to-drag (L/D) ratio delta planform configuration to the NASA space shuttle, as detailed in the article "A Delta Shuttle Orbiter" in the January 1971 issue of *Astronautics and Aeronautics*.⁷ Figure 5 shows the array of delta planform configurations the AFFDL considered during the 1958-68 timeframe.

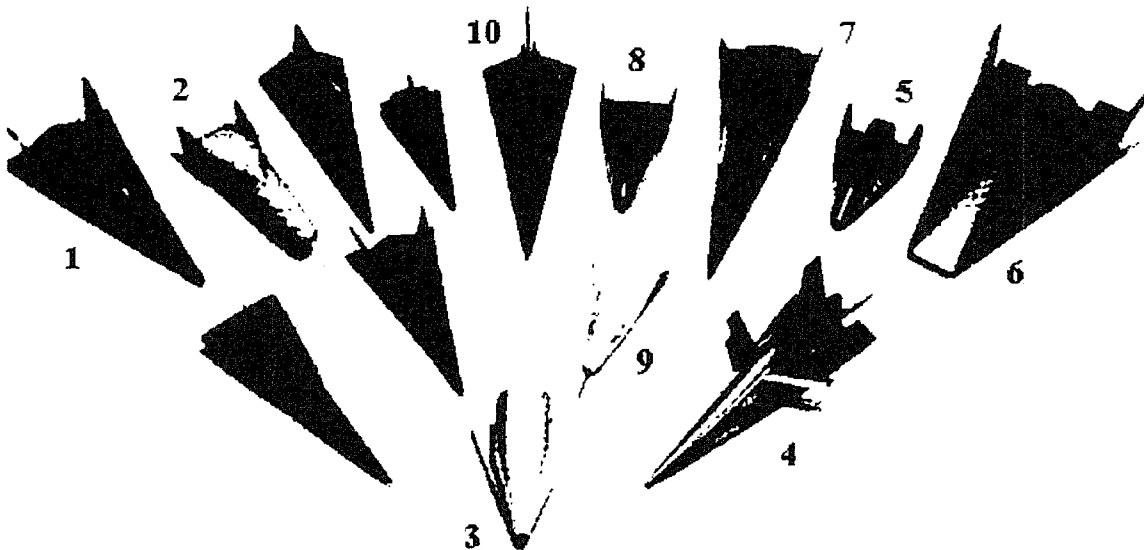


Figure 5. Delta-Lifting Body Designs. Array of delta-lifting body designs shows configuration is not limited to high hypersonic lift-to-drag ratios, high cross range, and large size.⁸

The AFFDL's approach was to design a hypersonic performance configuration that would minimize the waiting time in orbit to return to the continental United States (CONUS). This resulted in configurations with sharper leading edges and smaller nose radii than found in NASA and Russian configurations. All of the material, structural, and thermodynamic details related to the sharper configurations were tested and verified in ground test facilities and flight tests (BGRV and ASSET). Characteristics of selected AFFDL hypersonic glider configurations are identified in Table 1.

Table 1. Characteristics of Selected Flight Dynamics Laboratory Hypersonic Glider Configurations During the 1958-68 Timeframe

#	Model	Observation
1	FDL-24B	Flat bottom, sharp leading edges, conventional tails, as designed
2	All Body Glider, similar to Russian BOR vehicles	Upturned spatular nose, conventional tails
3	ASSET	Test vehicle to evaluate aerodynamics, thermodynamics and materials, based on nose of DynaSoar
4	FDL-7MC	Flat bottom, sharp leading edges, variable geometry wing, experimentally developed tail X configuration
5	Blunt nose, wing-body	DynaSoar type configuration
6	Spatular Nose Version of DynaSoar type	First integration of 2-dimensional nose (less drag) on a hypersonic glider (R.D. Newmann)
7	FDL-8	Flat bottom, sharp leading edges, outboard tails
8	HL-10	NASA Ames flat up-swept with bottom, round upper body, high dihedral angle tails
9	X-24A	NASA Langley round body, high dihedral angle tails
10	Star Body	based on Russian Star Body type configuration

Configuration 2 was a higher wing-loading, relatively blunt all-body with an upswept spatular nose that is not unlike Russia's Bor series of Lozino-Lozinski hypersonic gliders. When the author was at Wright-Patterson, interest in this waned quickly because of the limited cross range available. Because of the longitudinal extent of the former Soviet Union compared with the United States, the minimum L/D ratio to ensure a landing on the continental land mass was less for the former Soviet Union than it was for the United States—1.7 for the Soviet Union versus 2.7 for the United States.

Configuration 3 was a subscale research vehicle to evaluate the thermodynamic and materials for hypersonic gliders. The nose and leading edge radii were full-scale size. ASSET was successfully flown on a Thor intermediate-range ballistic missile (IRBM) booster. One that was recovered after an ocean landing is on display in the U.S. Air Force Museum in Dayton, Ohio. Configuration 6 was the first two-dimensional nose applied to a conventional winged-body (configuration 5) in the United States.

Configuration 4 was a product of cooperation between the AFFDL (Alfred Draper) and McDonnell Douglas Astronautics Company (Robert Masek) to develop a vehicle to support the Manned Orbiting Laboratory (MOL). This concept was briefed to the U.S.

Air Force in 1964, and elements of that configuration will be shown later. The intent was a 9- to 12-person vehicle for crew rotation that could alternatively carry supplies to the orbital station on a regular, frequent schedule (about one flight per week per vehicle). The variable geometry switchblade wing permitted landing with heavy loads returning from space and eventually horizontal takeoff. The experimentally determined configuration feature was the tail configuration. This configuration was wind tunnel tested and demonstrated inherent stability and control at speeds ranging from mach 22 to landing speed.

Configuration 6 was a product of cooperation between the AFFDL (Richard D. Neumann) and McDonnell Douglas Astronautics Company (Robert Krieger) to reduce the drag of hypersonic gliders. Based on the physics that a two-dimensional wedge has less drag than a right circular cone of the same volume, these engineers devised the "spatular leading edge." The wind-body configuration formed the basis of the X-20 and DynaSoar configurations that had a limited hypersonic L/D ratio, primarily because of drag. With the spatular nose, the nose wave drag could be reduced by 35 to 40 percent, thus increasing the hypersonic L/D ratio. Configuration 6 was derived from the conventional wing body, configuration 5.

Configuration 10 is an adaptation of the Russian "Star Body" concept that can enter in one of three orientations and need not always have one side facing the flow (compression side). The theory was that in a damaged situation, one of the three sides would be available for a safe entry. The limitation of this configuration concept is a small internal volume and a high ratio of wetted (surface) area per planform area that reduces the hypersonic L/D ratio.

The X-24B was based on the FDL-8 configuration. The different approaches to hypersonic glider configuration are best exemplified by Figure 6. The X-24A, built by Martin Marietta at its Denver, Colorado, facilities, is a round fuselage configuration with outboard high-dihedral-angle vertical tails. All the configurations of this type have serious lateral-directional stability problems at low speeds and tend to roll about the horizontal axis through the fuselage. One designer, the Russian Glebe Lozino-Lozinski, solved the problem by employing variable dihedral tails. The AFFDL solved the problem by using nonround configurations; that is, the quest for high hypersonic L/D ratios led to the solution of the low speed problem. Under an AFFDL program, Martin Marietta modified the X-24A into a flat-bottomed configuration with trailing edge elevons called the X-24B, shown in Figure 6. Comments by Bill Dana, the NASA pilot who flew the X-15 and the X-24A/B, about the change in the slow speed performance of the X-24B confirmed the advantage of the AFFDL approach.⁹

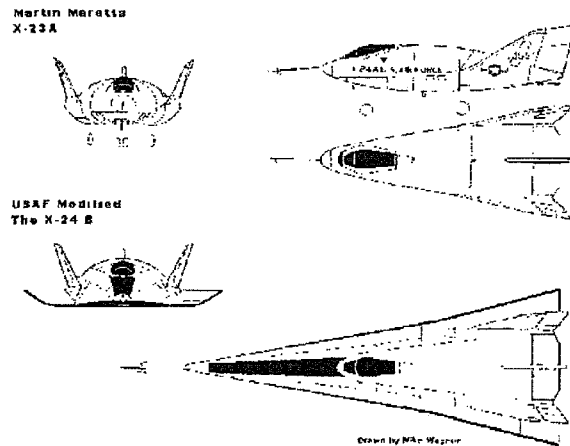


Figure 6. Martin Marietta X-24 A & B Research Gliders. X-24A based on USAF PRIME configuration.

The design parameters that largely determine a spacecraft's weight are its configuration and the amount of wetted or surface area relative to the planform area. The hypersonic gliders shown in Figure 5 have differing values of wetted area to planform area. Another important factor is the presence of wings, such as for configurations 5 and 6, which are wing bodies with a relatively thin wing or no wing, such as the lifting-body FDL-class hypersonic glider (configurations 2, 4, or 7). In this case the lifting bodies have a shape advantage that reduces the amount of surface area that is thin or subject to high heating. In the 1960s, when the U.S. Air Force's high-performance lifting body was competing with NASA's modest-performance wing body, there was much debate regarding the weight of these lifting concepts compared with that of a ballistic capsule (see Appendix A). At that time, with the large sea-recovery fleets, ballistic capsules were the only entry vehicles in either the United States or the former Soviet Union. A number of studies in the early-to-mid-1960s attempted to rectify and quantify the weight of a lifting entry vehicle compared with a ballistic capsule. In all the discussion in the Mercury, Gemini, and Apollo programs, the cost of the sea recovery was almost taken for granted, so the focus was on the cost of the vehicle itself, not the entire vehicle system. The government assembled a chart representing the relative weight of hypersonic entry systems—from ballistic to high-performance (high L/D ratio) gliders—collected from contractor and government reports. The relative weight was the system weight compared with that of a ballistic capsule with the same payload capacity. The result was a correlation curve that showed the high-performance wing-body gliders could weigh as much as twice what a comparable payload ballistic capsule weighed. This correlation was based on the L/D ratio of the vehicle. Apollo has an L/D ratio of about 0.5, but the system was still a ballistic vehicle with a very limited cross range. One correlation of the data is:

$$W/W_0 = 1 + 0.1259g(L/D) - 0.1029g(L/D)^2 + 0.0621g(L/D)^3 \quad (2)$$

W_0 = the weight of a ballistic capsule with the same payload

This correlation yields a high hypersonic L/D ratio glider with a weight almost twice that of the ballistic capsule. In this correlation, different configuration concepts were mixed and correlated as a single data set. A report cited in Appendix A (Stephens, 1965) concluded, "Weight factor for lifting spacecraft results primarily from larger surface area and only secondarily from the associated spacecraft environment and may be as large as a factor of two greater than ballistic spacecraft."

Engineers at the McDonnell Douglas Astronautics Company examined the database and concluded the large weight impact for a lifting spacecraft was as much a function of the configuration as the L/D ratio. The engineers set out to separate the database into families of like configurations. Where gaps existed, they established a configuration that provided the L/D ratio sought that was based on the configuration rules for that family. Three families were identified. The SV family configurations were based on circular/elliptical cross-section configurations that were characteristic of the HL-10 and X-24A NASA configuration concepts. The FDL family configurations were based on the trapezoidal delta planform configuration. And the MRS family configurations were based on a McDonnell Douglas modified version of the FDL family, with an emphasis on creating metal-radiative thermal-protection shingles that were flat, thereby reducing the cost of the shingle and perhaps introducing an element of hardware interchangeability. Altogether, 10 configurations from among the 3 families were

designed, weighed, and performed using the same industrial fabrication capability. The result was a curve representing each configuration family, as shown in Figure 7. The three families are represented by the three parallel straight lines.

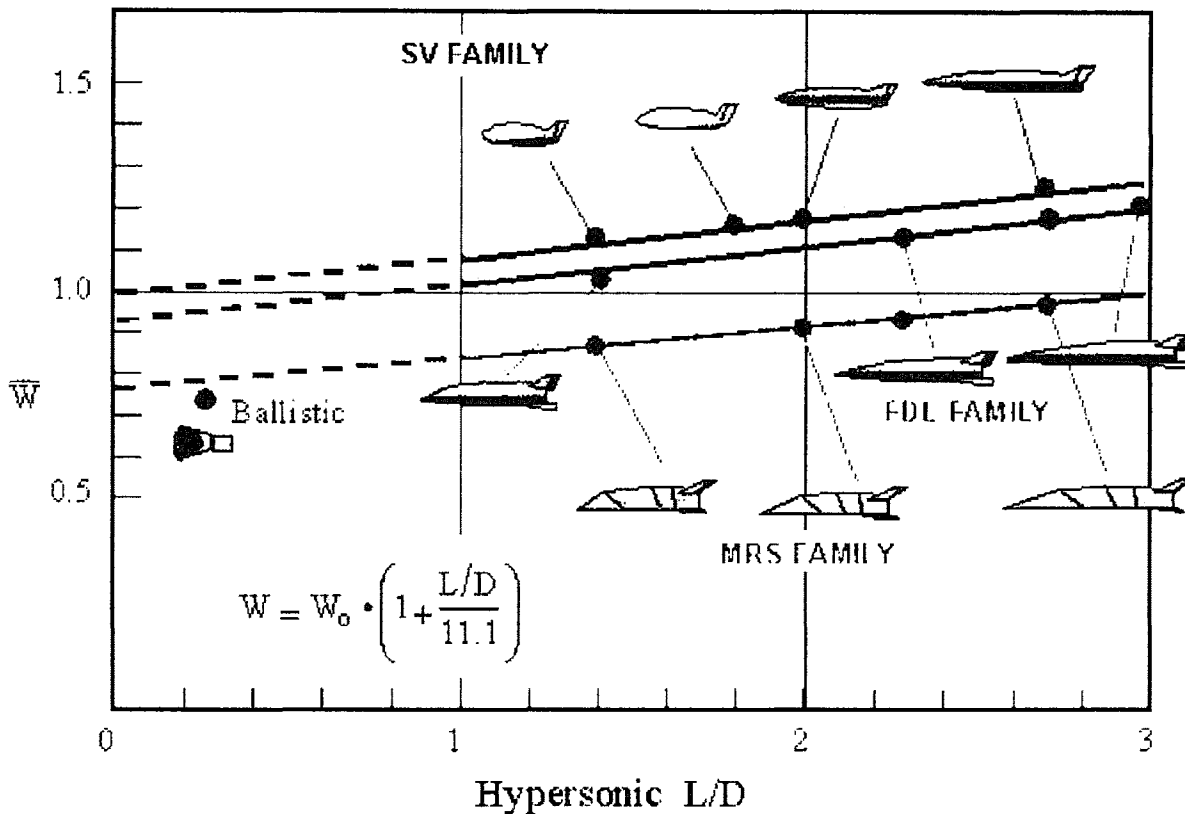


Figure 7. Detailed Design Analyses Show the Weight Trends are as Much a Function of Configuration Family as Lift-to-Drag Ratio

$$\begin{aligned} W/W_0 &= K_g \left[1 + 0.0901g(L/D) \right] \\ K &= 1.000 \quad \text{for the SV Family} \\ K &= 0.9297 \quad \text{for the FDL Family} \\ K &= 0.7622 \quad \text{for the MRS Family} \end{aligned} \tag{3}$$

This illustrates that the configuration and its individual wetted area to planform area can vary as much in their spacecraft weight as they can in their L/D ratio. The high L/D-ratio configurations had weights comparable to same-payload ballistic capsules of:

$$SV = 1.9 \qquad FDL = 1.7 \qquad MRS = 1.4$$

So the penalty for having a lifting-body configuration is less than expected if the configuration characteristics are taken into consideration in the design and weighing of the spacecraft. In addition, the reason the lifting spacecraft with high performance was considered was to eliminate the need for sea recovery and therefore the cost of a recovery fleet and the damage incurred by the spacecraft in a saltwater landing. The

goal was to be able to recover the spacecraft at any airport in CONUS, to eliminate the need for an overseas recovery site, and to eliminate the waiting required until a lower L/D ratio could land in CONUS (up to 14 orbits for the Apollo capsule, or 21 hours). In an emergency, that may be too long. The AFFDL's goal for the spacecraft to support the Manned Orbiting Laboratory was no waiting but to be able to reach CONUS from any arbitrary MOL position in its orbit. This was considered possible in the 1964-65 briefs to the government with respect to MOL, specifically the Model 176 configuration the MDC proposed for the MOL support in 1964.

The hypersonic glider based on the FDL-7C and the hypersonic air-breathing aircraft in Figure 8 both have hypersonic L/D ratios in excess of 2.7. In very practical terms, that means unpowered cross ranges in excess of 4,500 nautical miles and down ranges on the order of the Earth's circumference. So these two craft can depart from any location of a low-altitude orbit and land in CONUS or in continental Europe. Both are dynamically stable over the entire glide regime.

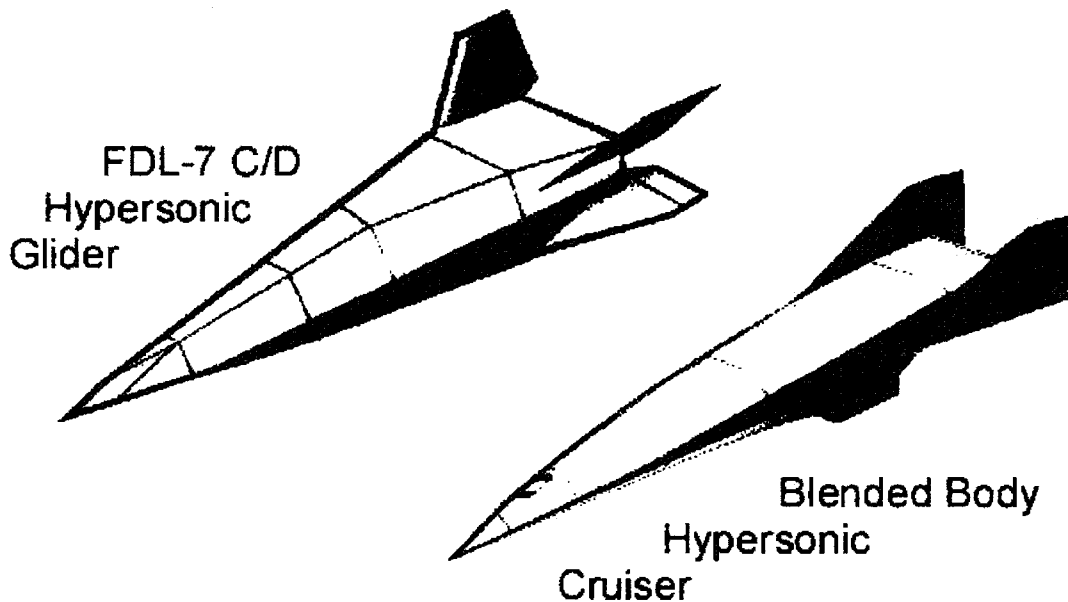


Figure 8. High-Performance Hypersonic Glide Aircraft. Rocket boost-glide and air-breather cruiser.

The wing-body, cylindrical fuselage advocates have strongly criticized the lifting bodies, contending that they are poorer configurations and much more complicated than the conventional-wisdom wing-body configurations (see Figure 9). However, that is far from the truth. The structural specialist sees this configuration as a lightweight propellant tank and assumes it is this consideration that drives the design. Rather, that observation introduces problems for all other technical disciplines that are far more difficult to rectify than a noncylindrical tank or a cylindrical tank in a nonsymmetrical cross section. The lone lifting surface with trailing edge controls introduces control issues just as it did for the space shuttle.

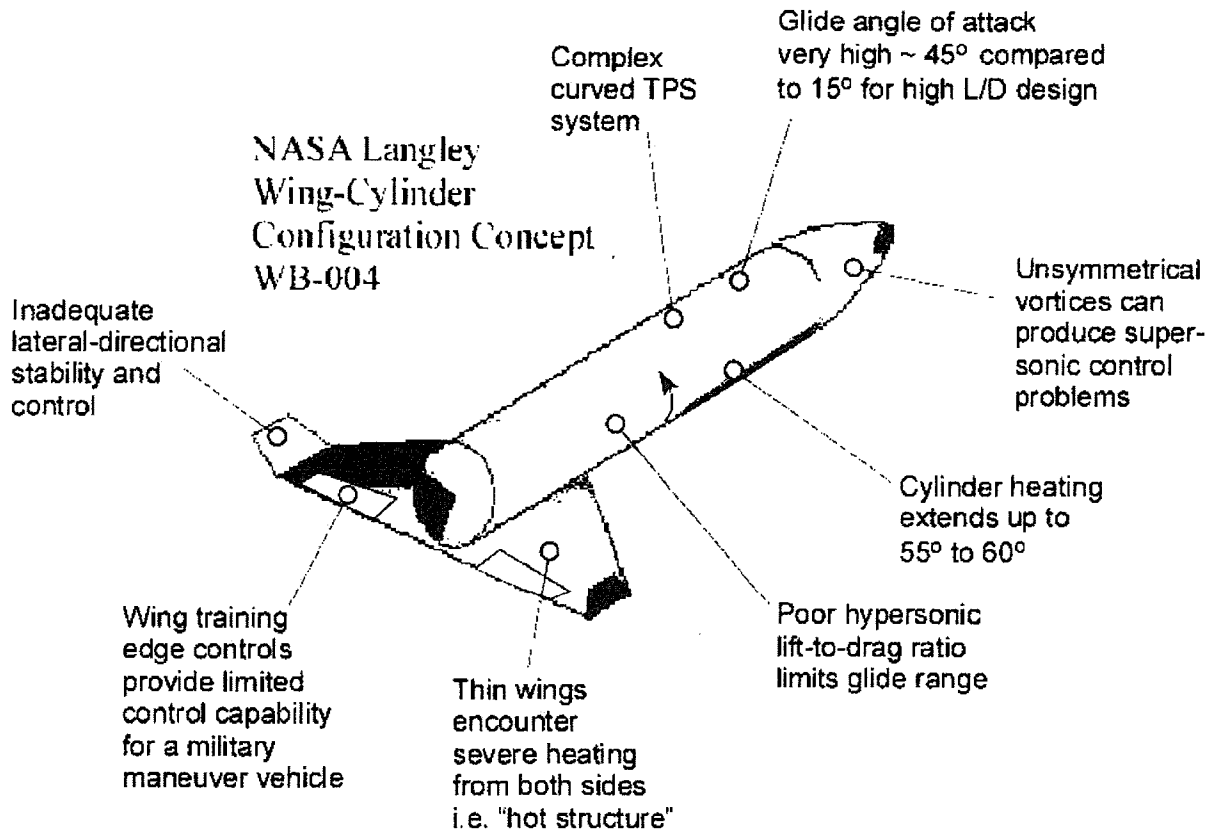


Figure 9. NASA Langley Wing-Body Configuration WB-004 With Generally Critical Areas for Wing Bodies Identified

With a high entry angle of attack, the cross flow over the cylinder produces high heating rates beyond the mid-cylinder line. With a lower L/D ratio, the down and cross ranges are limited as to what might be achieved but more in line with NASA one-missed-orbit criterion. The thin wings are heated on both sides to create added thermal problems, as well as added surface area to increase drag.

Al Draper and his team, together with Bob Masek's team at McDonnell Douglas Astronautics, worked long and diligently to arrive at the FDL-7/Model 176 configurations shown in Figure 10. The insert photo is Dale Reed's model of the FDL-7MC radio-controlled model at NASA Dryden. The AFFDL and MDC configurations were inherently stable at all operational angles of attack from at least mach 22 to landing speed. The remainder of this report will focus on the characteristics of this class of lifting body. The statements in Figure 10 were all based on wind tunnel data. A real advantage of the trapezoidal shape was not only flat metallic shingles but heating on the sides and upper surface that was at least three-fifths that of the conventional shapes. The glide range was such that this configuration could land in CONUS from any location on any inclination orbit from its current orbit with no waiting.

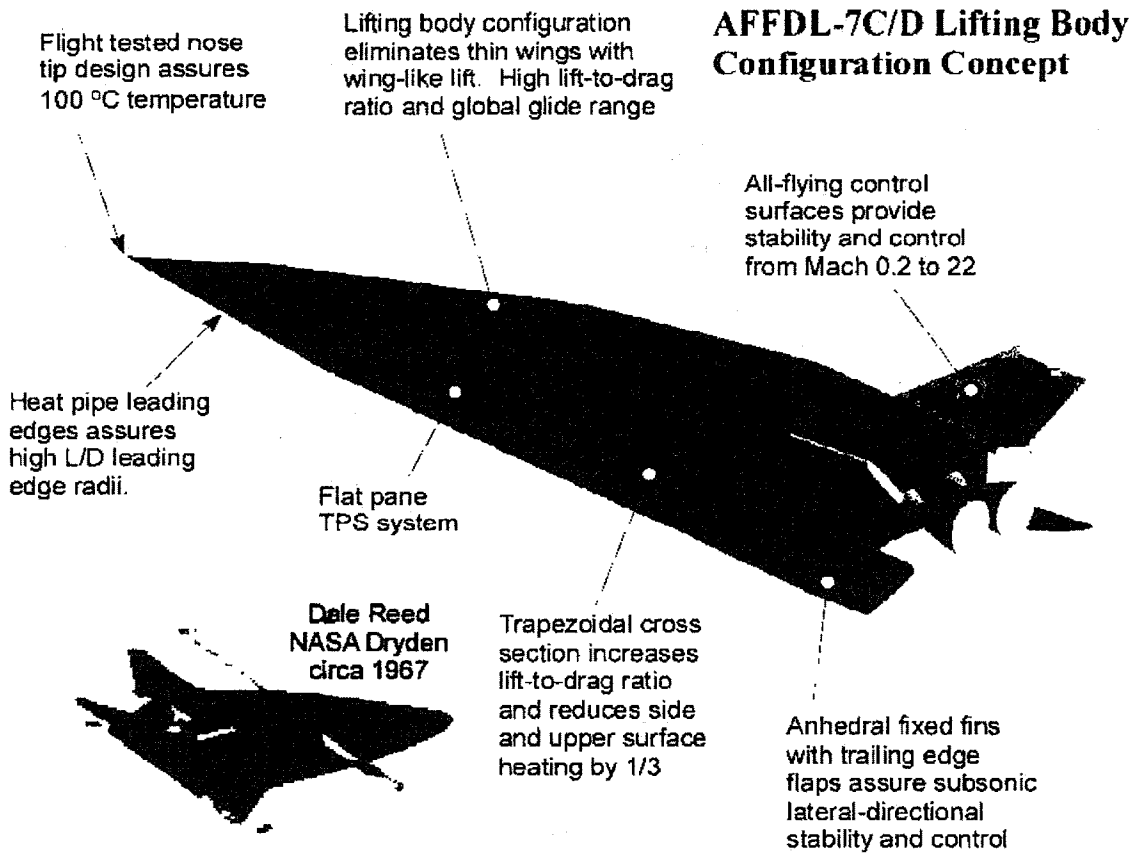


Figure 10. FDL-7C/D and FDL-7MC Lifting-Body Configuration. Offers inherent stability and control with sufficient volume and high lift-to-drag ratio.

The switchblade wing version of the FDL-7MC was the preferred version for 1983 studies that were part of the McDonnell Douglas TAV (transatmospheric vehicle) effort; that vehicle was powered by either an Aerojet Sacramento air turboramjet or an air-breathing rocket propulsion system. The inward-turning, variable-capture area inlet¹⁰ provides the correct engine airflow from landing speeds to mach 5.5, as illustrated in Figure 11.

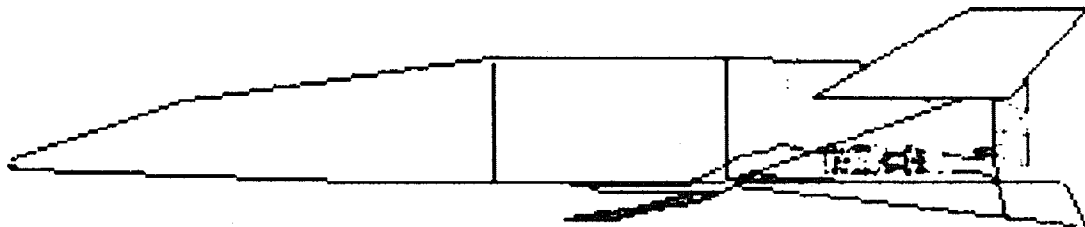


Figure 11. FDL-7C/D with a DuPont Retractable Inward-Turning Inlet

The propellant tanks were cylindrical-segment, multilobe structures with bulkheads and stringers to support the flat, metal-radiative thermal-protection shingles (very similar to those fabricated by Goodrich Aerospace for the now-defunct X-33). The nose was

transpiration cooled with a low-rate water-porous spherical nose. The sharp leading edges (the same leading edge radius was used for the nose tip) were liquid-metal heat pipes. This approach was tested successfully during the 1964-68 timeframe and was found to be equal in weight and far more durable than a comparable ceramic tile/carbon-carbon system. The AFFDL's experience with carbon-carbon leading edges on the ASSET test vehicle convinced the Air Force it needed a more durable solution.

Figure 12 compares the FDL-7C/D and the McDonnell Douglas Model 176. The Model 176 had a power law nose that was essentially a curved spatular nose and a higher sweep angle, resulting in the same usable volume but with a higher hypersonic L/D. Sacrificed were the flat-panel thermal-protection shingles over part of the fore body. Both configurations retained the X-tail configuration developed by Gil Gaumer of McDonnell Douglas. At the time, the launch vehicle would have been a Martin Titan IIIC. Had an engine with the performance of the Pratt & Whitney XLR-129 been available, there would have been lateral recoverable, fuel/oxidizer tanks on either side of the vehicle, with all of the engines installed in the hypersonic glider. This was similar to the Lockheed Star Clipper (see Figure 38).

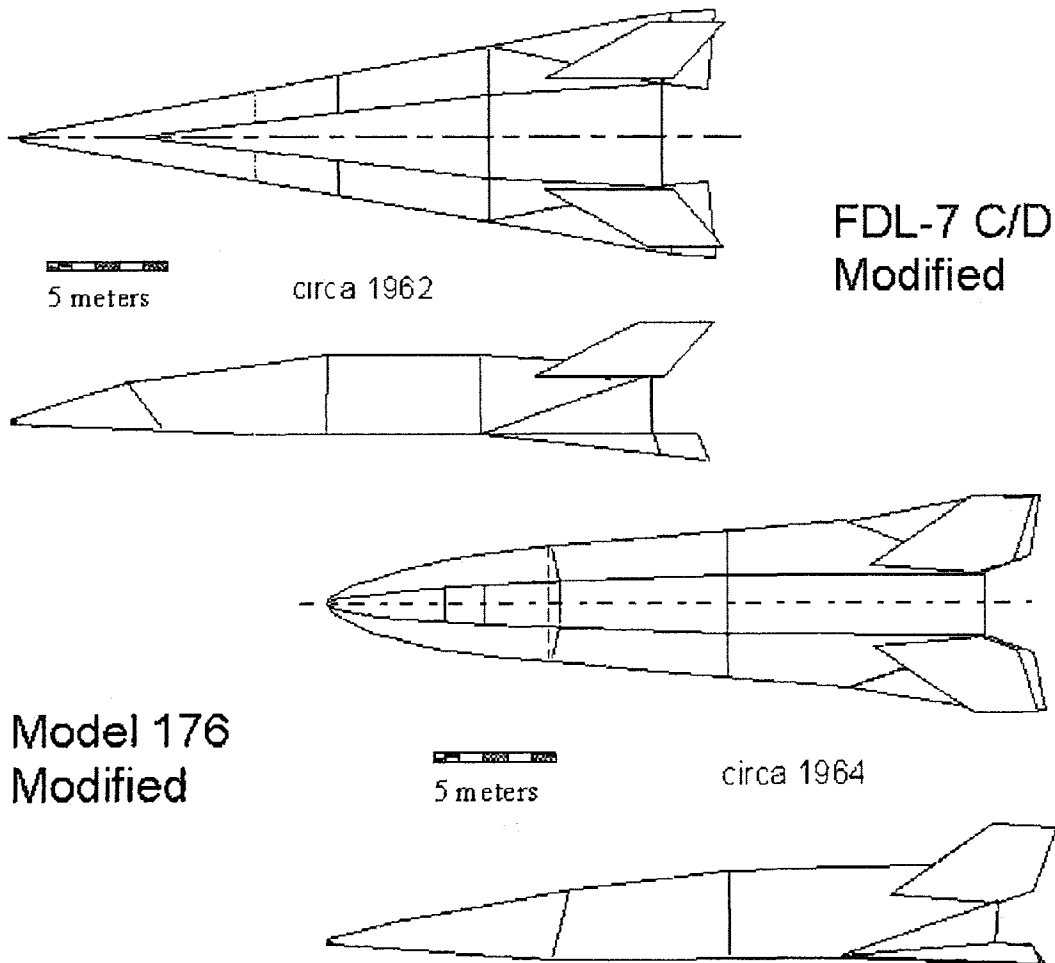


Figure 12. Comparison of FDL-7C/D (top) and Model 176 (bottom)

The author was aware of three people—James S. McDonnell, the AFFDL's Albert Draper, and Russia's Glebe Lozino-Lozinski—who clearly understood the need for a long cross-range and down-range capability, not just for one missed orbit. Critics will observe that Lozino-Lozinski had limited his BOR vehicles to an L/D ratio of 1.7 to 1.8 and not the 2.7 to 3.0 required for Earth circumferential glide range. First, the longitudinal extent of the former Soviet Union was twice that of CONUS, and an Earth circumferential glide range was not necessary to ensure recovery within the continental Soviet Union; therefore, a lesser L/D ratio was acceptable. Second, in personal conversations with the author, Lozino-Lozinski indicated a Russian government agency forced him to limit the glide range to ensure recovery in continental Russia and prevent escape to the United States. In a further step to prevent escape, when the vehicle was in range of CONUS, ground control disabled its deorbit system.

The need for a long cross-range and down-range capability so there is no waiting in orbit in the case of an emergency or military need is presented graphically in Figure 13. Interestingly, the greatest lateral-range (cross-range) requirement for no waiting is for 55° orbital inclination, the usual Russian orbital inclination. The nominal U.S. orbital inclination is 28.5 degrees, with a waiting time of 8 orbits (approximately 12 hours) for a space shuttle-class glider. At the International Space Station orbital inclination, the orbital waiting time for a shuttle-class glider is 6 orbits. In comparison, Apollo's orbital waiting time was about 14 orbits, provided the return trajectory included an Earth-parking orbit before entry into the Earth's atmosphere. The FDL-7 and Model 176 class of gliders could immediately enter a return glide from their orbits. This provides a significant advantage for the International Space Station operators and vehicle crew, who need only enter hypersonic gliders attached to an orbital station and initiate deorbit procedures to be on the ground in less than 90 minutes in an emergency.

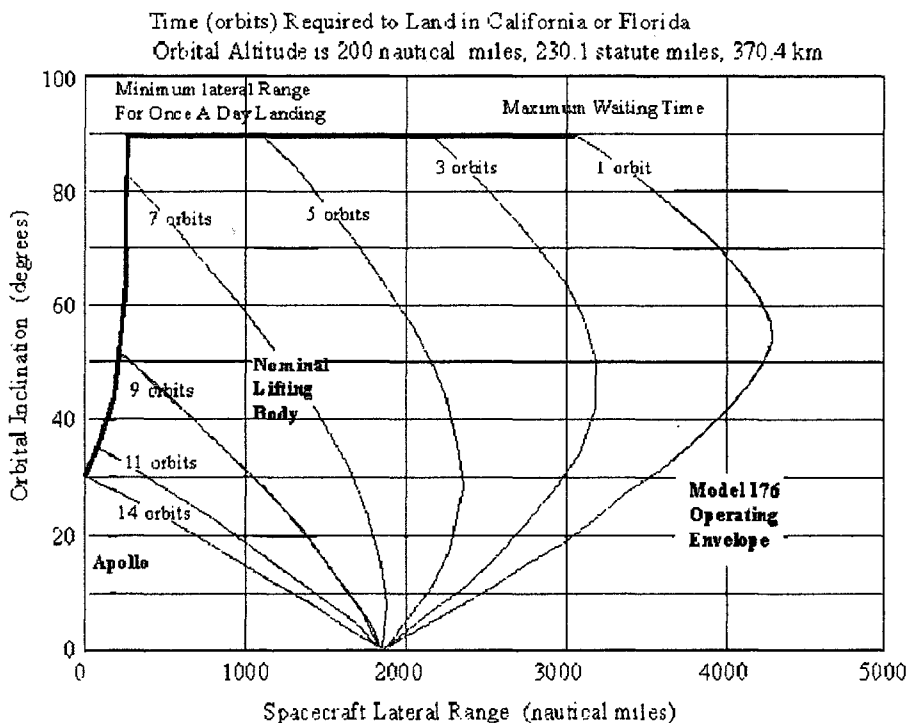


Figure 13. Sufficient Cross Range (L/D) Means There is No Waiting to Return

Figure 14 compares the glide ranges and L/D ratios of selected hypersonic gliders. The shuttle would be in the area of the nominal wing body on the righthand chart. From Figure 13, the no-waiting cross range (lateral range) is 3,600 to 4,400 nautical miles. That means the hypersonic L/D ratio needs to be in the 2.7 to 3.2 range. Appendix D has down and lateral ranges shown as landing ellipses. The key to a successful landing is a subsonic L/D ratio that is in the 4.5-or-greater range. The NASA round-bottom configurations were not capable of that subsonic L/D ratio. The X-24B was in that category and was therefore easily landed compared with the X-24A or Prime vehicles. These high-performance gliders were unique to the AFFDL. The intent in case of a fire would be to immediately evacuate to the hypersonic gliders and then depressurize the station to control any fire (remember that Mercury and Gemini could be depressurized). A crew could then be launched to recover the operation and repair the station.

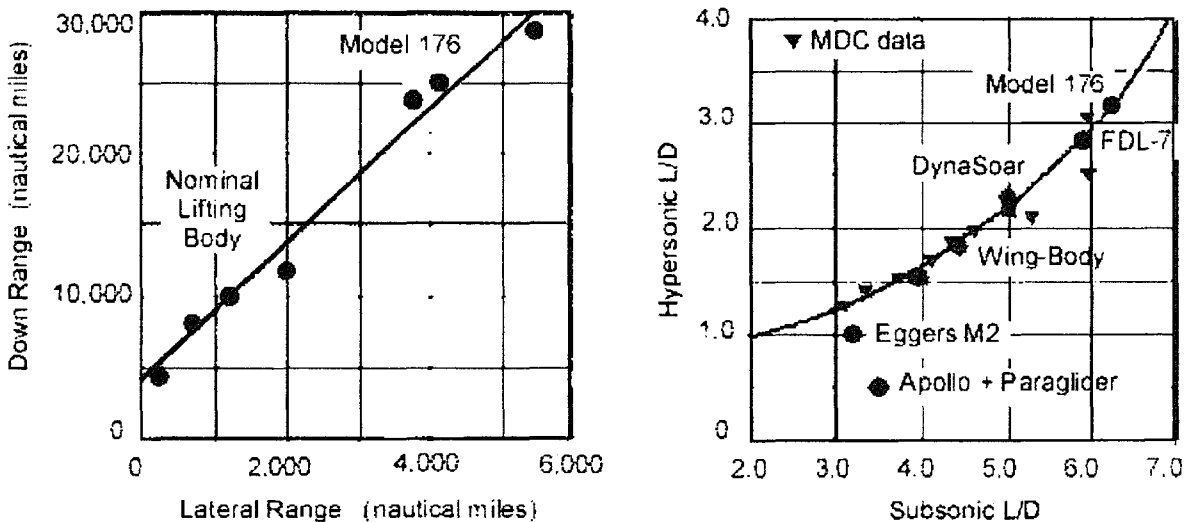


Figure 14. Hypersonic Glider Characteristics

There is always the question about landing these blended bodies. Figure 15 shows the blended body handling qualities to be very good, and therefore a pilot's fear factor is less than with the X-15. Bill Dana said the X-24A was difficult to handle when landing but that he could land the X-24B almost with no hands as it flared automatically. To the author's knowledge, all of the wind tunnel tests showed inherent static and dynamic stability over the entire speed range.

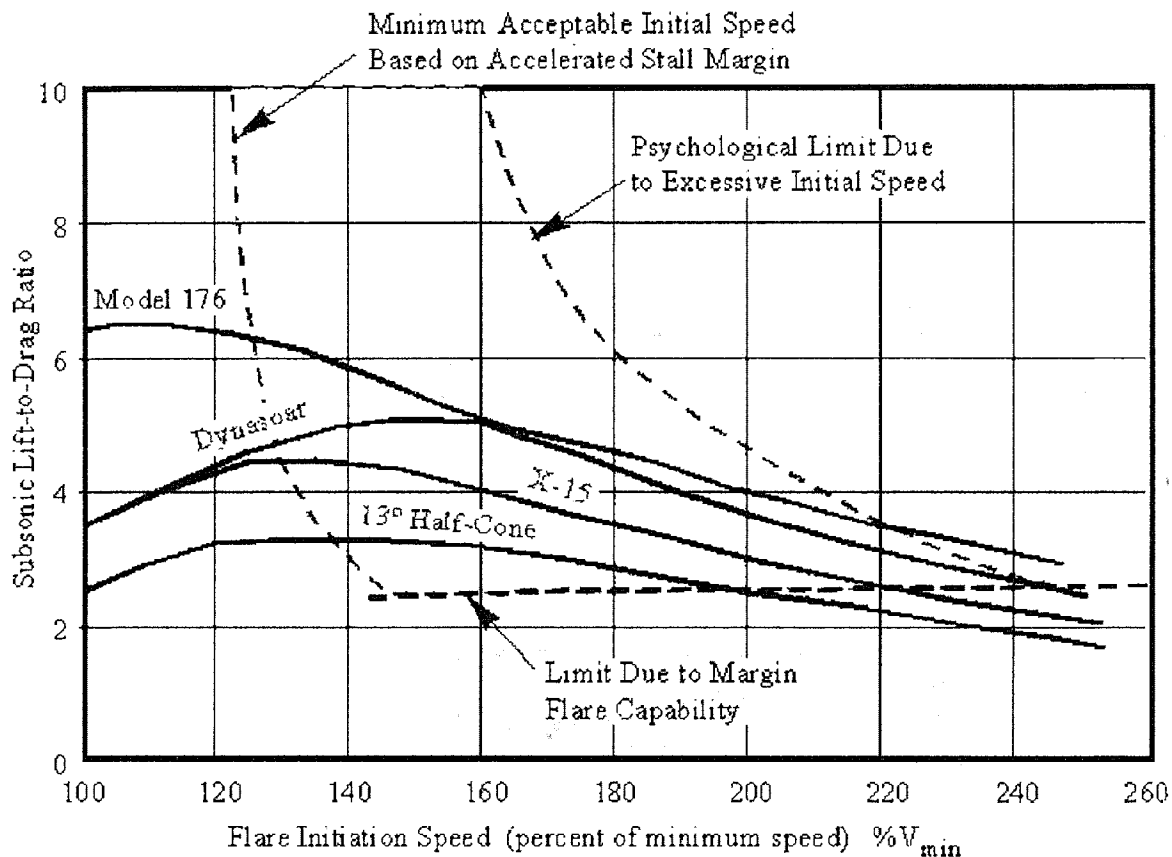


Figure 15. Both Delta Planform Lifting Body (Dynasoar) and Model 176 Offer Superior Landing Performance

Thermodynamics and Materials

The structure of Model 176 was based on diffusion-bonding and super-plastic forming of flat titanium sheets. Forty years ago, the method was called "roll bonding" and executed with the titanium sealed within an evacuated steel envelope and processed in a steel rolling plant. With a lot of effort and chemical leaching, the titanium part was freed from its steel enclosure. All of that has been completely replaced today by the current titanium diffusion-bonding and super-plastic forming industrial capabilities. The photo in Figure 16 is from a Society of Automotive Engineers book titled *Advanced Engine Development at Pratt & Whitney: The Inside Story of Eight Special Projects 146-1971*, by Dick Mulready. Chapter 6, "Boost Glide and the XLR-129 - mach 20 at 200,000 Feet," shows a surviving remnant from the 1960s program.

The super-plastic-forming, diffusion bonding that was so difficult in early 1960 is now an accepted fabrication procedure. One of the F-15's major bulkheads was fabricated from titanium sheet elements using this procedure instead of machining away more than 90 percent of a titanium forging. Had the procedure been adopted as a product-manufacturing method, it would have eliminated the almost 2-year manufacturing cycle in acquiring titanium forging of the wing spars and major bulkheads. Note that only 2.5 percent of the thermal heating enters the primary structure.

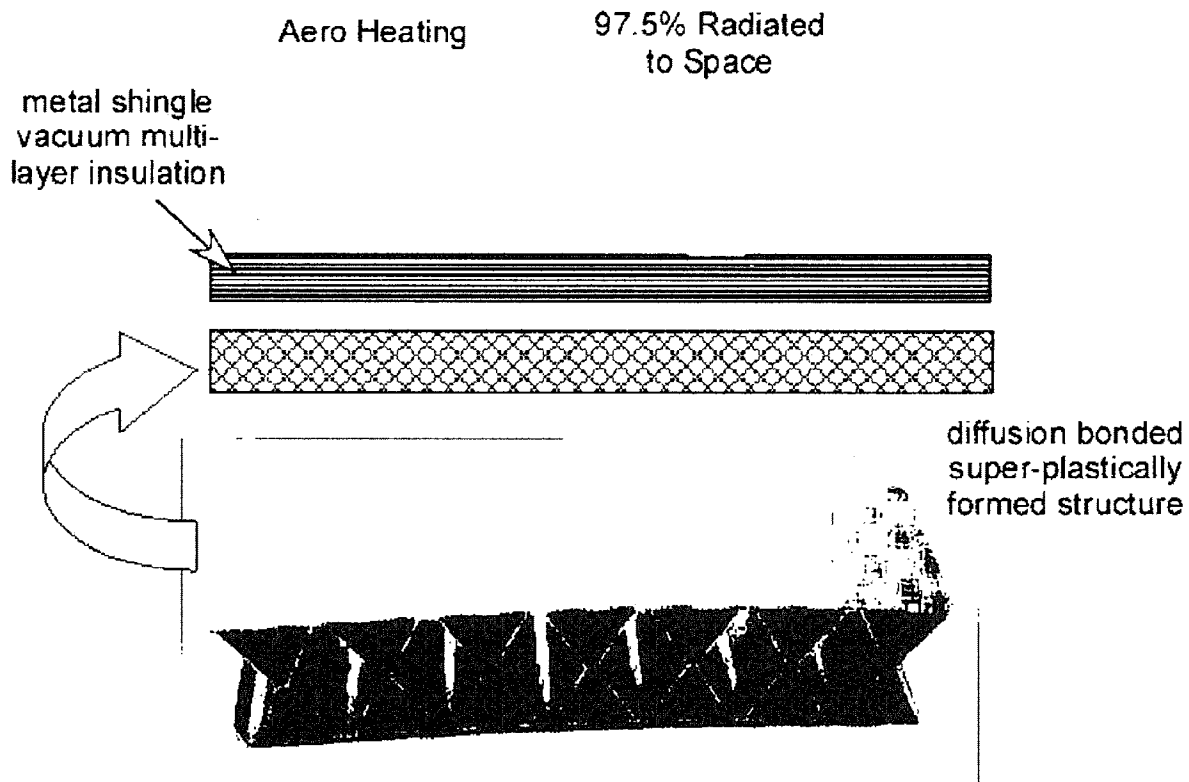


Figure 6.1. McDonnell titanium structure. (Courtesy of John Robson.)

Figure 16. McDonnell Aircraft Company Roll-Bonded Titanium Structure (circa 1963). Today this structure would be super-plastically formed and diffusion bonded from RSR titanium sheets.¹¹

Mulready's book mentions the McDonnell Douglas boost-glide strategic vehicle, as well as citing key personnel at McDonnell Aircraft Company. Low thermal conductivity standoffs set off the insulated-metal, thermal-protection-insulated shingles from this wall so that there was an air gap between them. The X-33 applied the metal shingle concept, albeit with significant improvement in the standoff design and thermal leakage, in the orientation, thickness, and weight of the shingles. This is one aspect of the X-33 that can be applied to future spacecraft for a more reliable and repairable thermal protection system than ceramic tiles. All efforts by the author to obtain information on the shingles manufactured by Goodrich Aerospace have been met with the response, "We lost the contract and are investing in more productive products." The titanium diffusion-bonded and super-plastically formed wall was both the primary aircraft structure and the propellant tank wall. The cryogenic propellants were isolated from the metal wall by a metal foil barrier and sealed insulation on the inside of the propellant tank. Significant testing of this structural approach confirmed its superior capabilities as a hypersonic radiation-cooled structure.

The Model 176 was proposed for the Manned Orbiting Laboratory. It was a thoroughly designed and tested configuration with a complete, all-metal thermal-protection system that had the same weight as ceramic tile and carbon-carbon concepts used for the U.S. space shuttle but was sturdier and could be repaired in a hanger or in orbit. A wind

tunnel model of the McDonnell Douglas Astronautics Company Model 176 installed in the McDonnell Aircraft Company Hypersonic Impulse Tunnel for a heat transfer mapping test is shown in Figure 17. Note that, conforming to the piloting concepts of the 1960s, it has a clearly distinct windshield. The model accomplished thermal mapping to determine the heat transfer distributions on the body and upper fins.

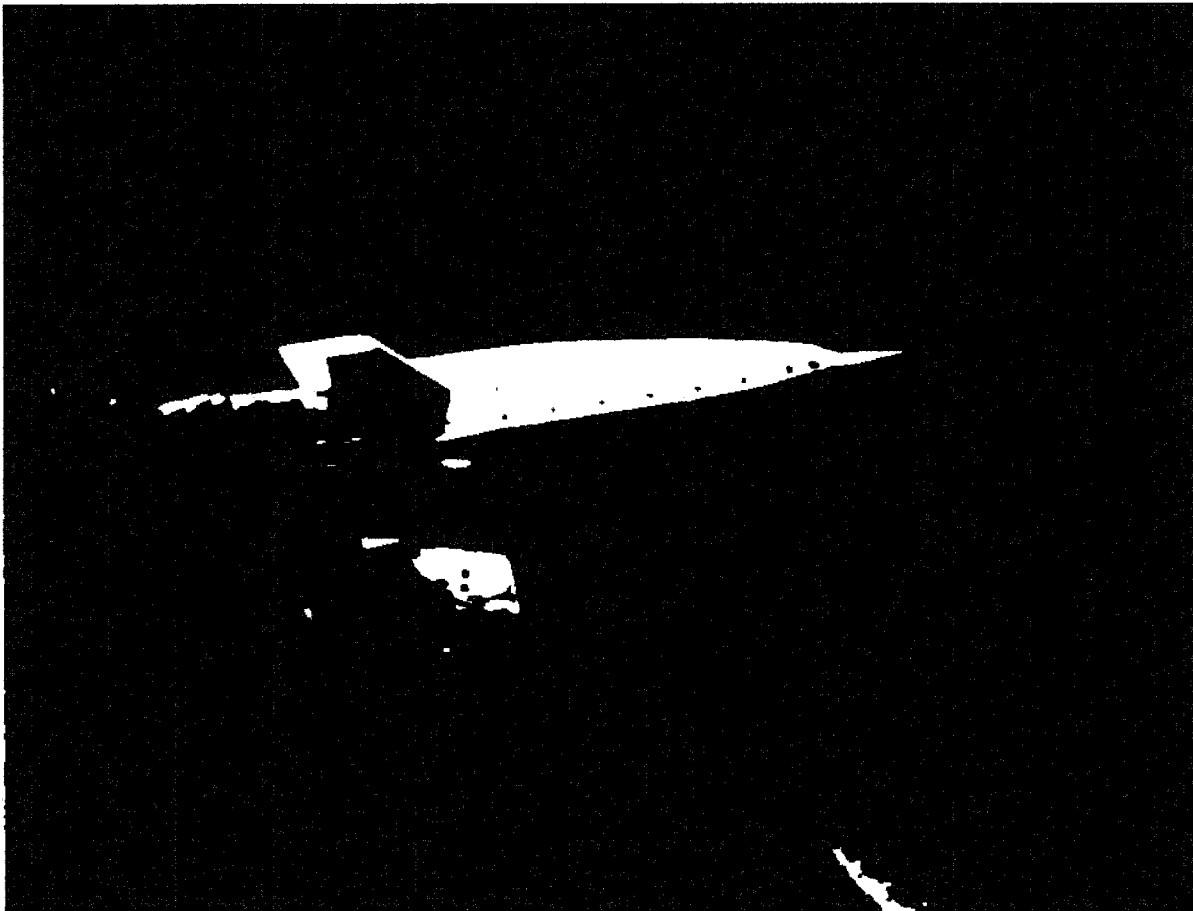


Figure 17. Model 176 in the McDonnell Douglas Hypervelocity Impulse Tunnel (circa 1964) for Thermographic Phosphor Heat Transfer Mapping, Including the Upper Fin.

Among the important determinations that resulted from these heat transfer tests was that the sharp-leading-edge, flat-bottomed, trapezoidal cross section reduced the heating to the sides and upper surfaces, as shown in Figure 18. In the range of angles of attack corresponding to maximum hypersonic L/D ratio, the sharp leading-edge corner separates and reduces the upper surface heating. Because of this separation, the isotherms are parallel to the lower surface and are 2,100 to 2,400 °F (1,149 to 1,316 °C) cooler than on the compression surface. The upper control fins are hot, but there are approaches and materials applicable to control surfaces. The temperatures shown are radiation equilibrium temperatures. With nose water transpiration cooling (demonstrated in a flight test in 1966) and heat pipe leading edges (demonstrated at NASA Langley in 1967-68), the temperatures of the nose and leading edges are 212 °F and 1,300 °F (100 °C and 704 °C), respectively. The thermal mapping enabled identification of primary flow characteristics in the boundary layer of the vehicle. In

Figure 18, radiation equilibrium skin temperature is the skin temperature that results when the radiated thermal energy stemming from the skin temperature equals the input aerodynamic heating minus any conduction into the airframe.

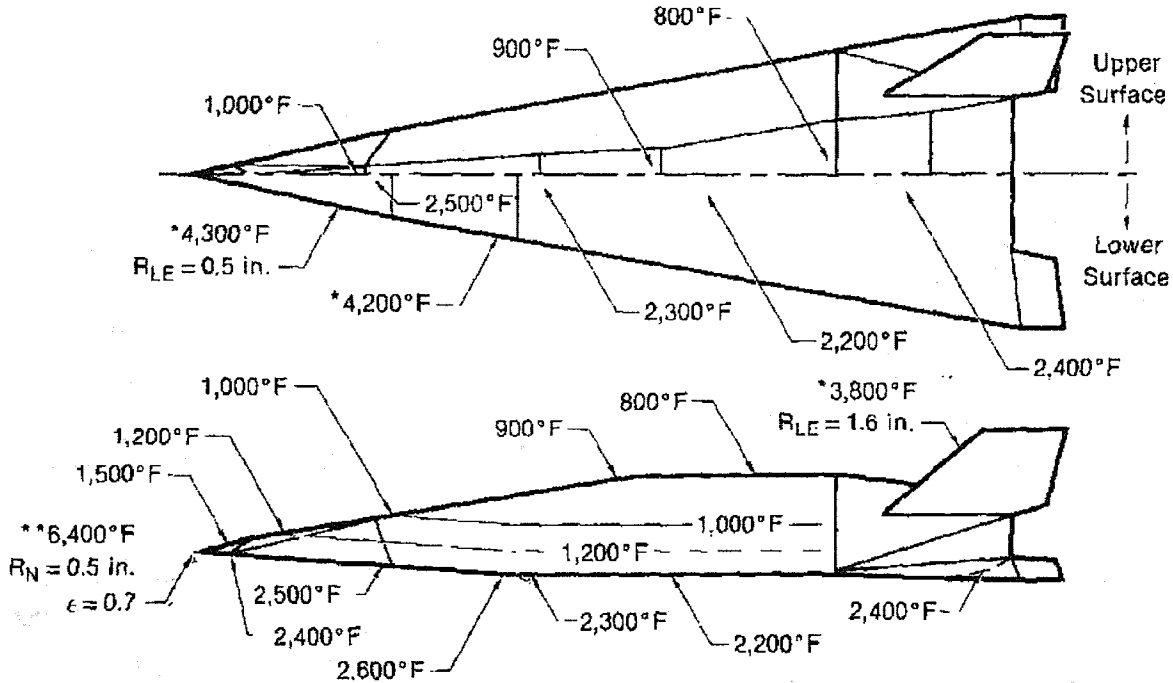


Figure 18. FDL-7C/D, Model 176 Entry Temperature Distribution. Upper-surface heating is minimized by cross-section geometry.

Figure 19 is a thermographic phosphor image of the model in Figure 17 at a 12-degree angle of attack (maximum L/D ratio) at mach 12. Even at mach 12, there are vortices embedded in the boundary layer. The three black dots are heat transfer gauges that were used to establish the value for q_{ref} in Figure 19. The stagnation heat transfer was 25 times the reference value. This technique, when calibrated with the reference heat transfer gauges, provided a rapid and accurate means to determine heat transfer distributions with a minimum of installed gauges. The technique was adopted by other wind tunnel facilities, including the Arnold Engineering Development Center at Tullahoma, Tennessee.

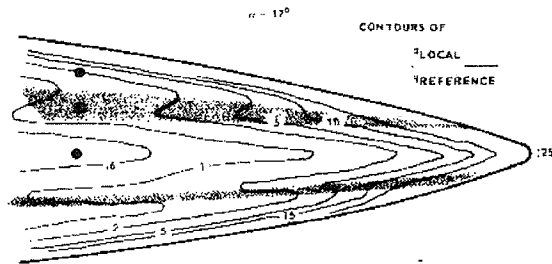


Figure 19. Even at Mach 12, Embedded Vortices in the Boundary Layer Alter the Local Heat Transfer

On other McDonnell hypersonic configurations with all-movable control surfaces, the interface between the fin and the body became a critical heating issue for the rotating shaft attaching the fin to the body. This was an area of concern on this vehicle, and specially instrumented fins were installed to measure the local heating. Again, the thermographic phosphors were used to map the heating. Figure 20 shows the model in Figure 17 at a maximum 48-degree angle of attack. Fin heating distributions were made at 16-, 24-, 34-, and 48-degree angles of attack¹² and are shown in Figure 21. The brighter the phosphor is, the lower its temperature is (the phosphor darkens as the surface temperature increases). So the area adjacent to the body is at a lower temperature than on the fin. In fact, examining Figure 21 shows that for all angles of attack tested, there was always the cool layer adjacent to the body. So the fin attachment journal/shaft would not be a thermal problem. At angles of attack lower than 16 degrees, the heating became less intense. This tail configuration of a fixed anhedral lower fin with trailing edge controls and an all-movable upper fin provided the control authority over the entire mach range required for stability and control and did not have a thermodynamic issue with fin attachment heating.

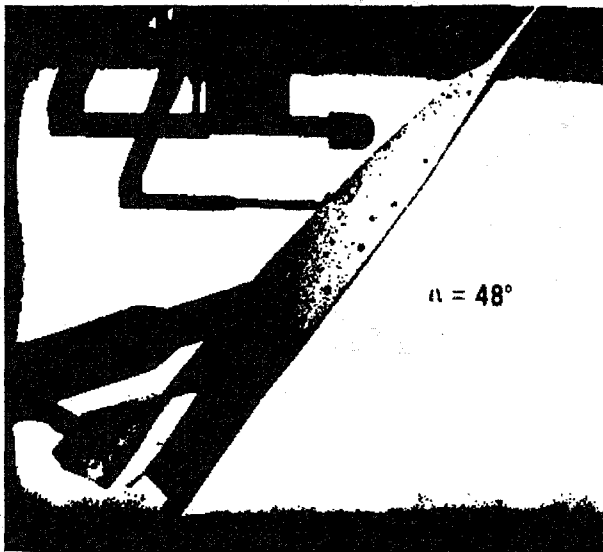


Figure 20. Thermographic Phosphor Image of Model 176 at Near-Maximum Angle of Attack

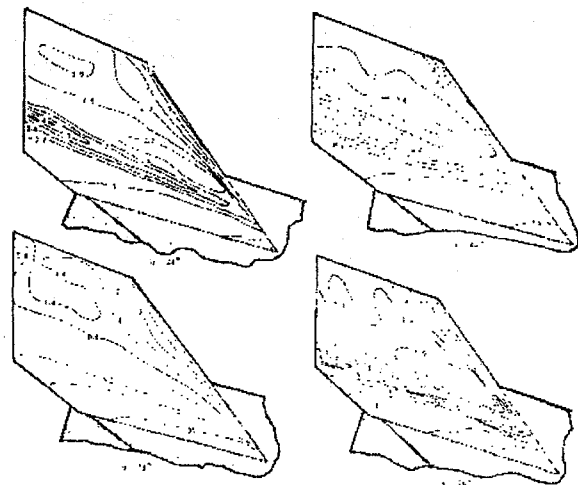


FIG. 6. ISODENSITRACER maps for lifting body tail fin for four angles of attack; contours show $q_{LOCAL}/q_{REFERENCE}$

Figure 21. From L/D Maximum to Maximum Angle of Attack, There is Always a Cool Sublayer Adjacent to the Wall

With 1960 materials and manufacturing methods, about 95 percent of the aerodynamic heating was radiated to space, about 2.5 percent was retained in the shingles, and about 2.5 percent was transferred into the titanium tank/primary structure. Using Goodrich Aerospace's standoff/attachment techniques developed for the X-33, today around 0.5 to 1 percent of the aerodynamic heating would be transferred into the titanium tank/primary structure. The shingle material would also be better today. Figure 22 shows a silicon carbide matrix reinforced with silicon carbide fibers that was shown at the 1988 Paris Air Show. A combustor of this material was operated at 3,000 ° F continuously for a number of days at SEP's Bordeaux plant, as witnessed by the author. Unfortunately, SEP was subsequently taken over by another company and promptly closed. The parts manufacturing at Bordeaux was truly impressive to someone in space systems but too costly to a subsonic round engine manufacturer.

One of the difficulties with silicon carbide (SiC) is that it is ridged fibers, like very-small-diameter rods. When the NASP team visited Japan in 1988, one of the very interesting products of the UBE Corporation was Tyranno[®] cloth (see Figure 23). Composed of strong, flexible fibers from natural Feldspar, Tyranno cloth handled and felt like tweed cloth. The cloth could be wetted by liquid aluminum or titanium, and the NASP team saw examples of both aluminum and titanium metal matrix composite (MMC) products. For example, an aluminum MMC piston and connecting rod was being used in Kawasaki racing engines. And a powder form of aluminum MMC was being used as a dry pigment that was fused onto the surface of Kawasaki motorcycle mufflers. The MDC NASP team foresaw many applications for Tyranno cloth for its NASP aircraft.

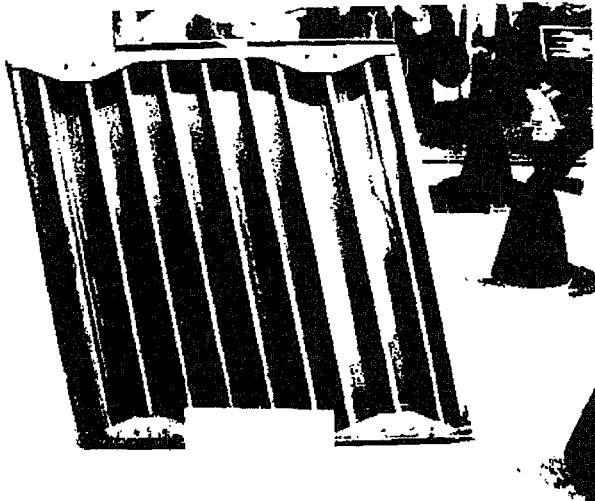


Figure 22. This 1988 SEP Bordeaux SiC/SiC Panel Could Sustain Temperatures of up to 3,000 °F. With SEP having subsequently closed, little of this capability remains.

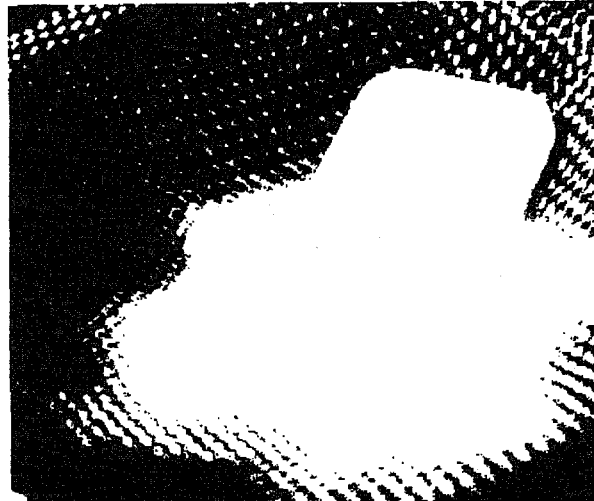


Figure 23. UBE Corporation's Tyranno Cloth. The cloth was used industrially in Japan.

The FDL-7 and Model 176 configurations always elicit comments that their sharpness and the associated high heating rates make them nonviable concepts. However, that is not the case. Figure 24 shows a 1-inch-diameter, sintered-nickel nose tip attached to a 1,000-psi water tank that sweats water. The result is a functional sharp, low-drag nose with a minimum-thickness entropy boundary layer.¹² This tip was flight-tested on a hypersonic glider (BGRV flight in 1966) beginning at about 22,000 feet/second. Today, Aerojet Sacramento's platelet diffusion-bonding technique would make this a much easier task. Some experimental evidence from the BGRV flight indicates the water vapor film in the boundary did act to reduce the heat transfer to the body aft of the nose.



Figure 24. A Porous Nickel Tip Oozing Water. This test lasted 4,300 seconds before the arc heater cathode—not the nose tip—failed.

AI Draper assembled the ASSET (Aerothermodynamic Structural and System Environmental Test) experimental flight-test program to evaluate current U.S. Air Force and NASA materials for hypersonic entry vehicles. The intent was to launch a test vehicle from an Air Force Thor IRBM in the 18,000 to 20,000 feet/second range and recover the vehicle. The ASSET glider was approximately the forward portion of the X-20 Dynasoar vehicle and is shown in Figure 25 after recovery. Except for the carbon leading edges, the materials generally performed as required. As a result, a small team of McDonnell Douglas Astronautics Company engineers and model builders began working on an alternative approach for the leading edges. This team's efforts resulted in the heat pipe leading edge shown in Figure 26, a series of formed stainless steel tubes brazed together to form a leading edge based on NASA space shuttle requirements. The tubes contained a stainless steel mesh wick and were filled with metallic sodium.

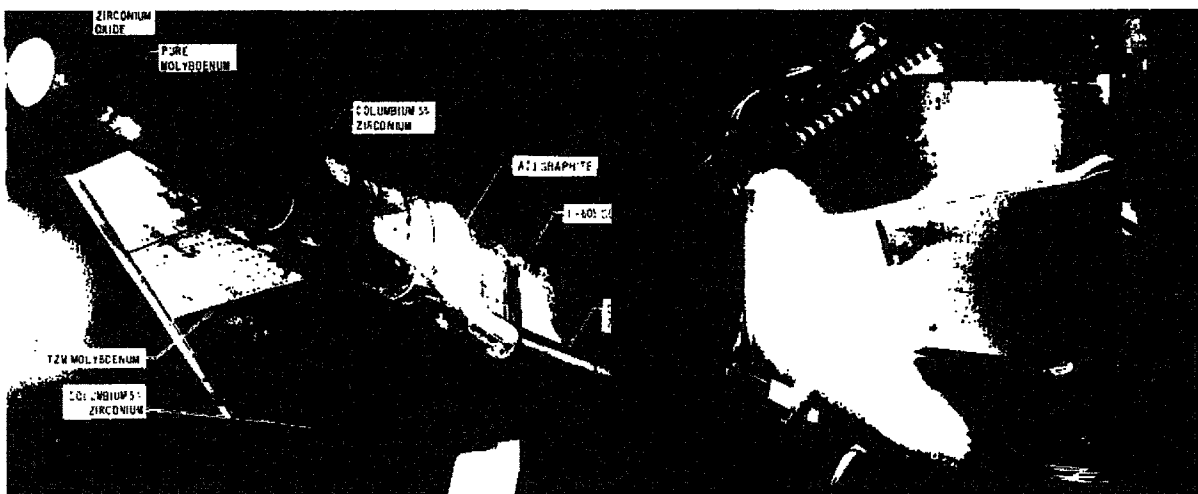


Figure 25. FDL ASSET Flight-Tested From Orbital Speeds To Evaluate 1960s' Materials. Carbon leading edges proved the least durable.

Figure 26. Heat Pipe Shuttle Leading Edge Designed and Built by McDonnell Douglas Astronautics. Tested extensively at McDonnell Douglas Corporation, St. Louis, and NASA Langley, it never failed.

The leading edge was tested in NASA Langley's 8-foot High-Temperature Structures Tunnel, the NASA Langley Radiation Thermal Test Facility and the McDonnell Douglas Graphite Thermal-Altitude Test Facility (graphite radiation heaters within a vacuum altitude chamber). All of these tests showed the installed leading edge to be durable, robust, and lightweight (equaled the installed NASA carbon-carbon leading edges). Starts from cold tubes showed the sodium melts and began the heat pump process without any difficulties. Because this leading edge was made by the engineers and mechanics as a one of a kind, the tubes developed thermal shorts and other problems over the span of the testing, all of which were rectified before the test continued. Although brittle and difficult to manufacture, this leading edge met the thermodynamacists' solution of a simple radiation structure, not a heat pump.¹³

The Qu Tube

In the 1990s, a colleague, Ying-Ming Lee, who then worked at MSE in Butte, Montana, showed the author a copper tube about a foot long that was a heat pipe from his colleague in Taiwan. If the tip was put into a cup of hot water, the other end almost instantly was too hot to hold. If it was quickly put into a glass of cold water, that tip just as quickly became ice cold. As documented in the excerpted page below from the University of Alabama, Huntsville, Annual Report, the apparent conductivity is greater than copper and could not be melted, as the thermal energy would be removed so fast that a significant temperature rise could not be attained. This could have significant industrial application for the United States. The late Clark Hawk had obtained a 10-foot-long Qu tube and tested it in his laboratory. The results were published in the University of Alabama, Huntsville, Annual Report. However, as Clark Hawk discovered, the Chinese team associated with Professor Qu in mainland China was not about to let this discovery into American hands. Plus his team was composed of a number of young, ambitious technocrats who thought they knew how to make their fortune. So both Ying-Ming's and Clark's attempts to advance beyond a demonstration tube ended in frustration. Any attempt to open the tube results in failure, as whatever is in the tube reacts into an inert powder. The author has two smaller tubes in his possession. With applications including hypersonic vehicles, nuclear power plants, and electronic cooling, these devices would lead to an economic breakthrough in practical thermal control.

the Qu Tube, or Supertube, is somewhat controversial. According to the inventor (Patent No. 6,132,823) and to claims by the company and their quoted results of tests conducted by Stanford Research Institute, it reportedly has an effective thermal conductivity of the order of 10 to 100 times greater than that of conventional liquid-vapor heat pipes, and over 30,000 times that of an equivalently sized solid rod of silver. Reports cited also have indicated puzzling temperature distributions can occur with these tubes, unlike conventional thermal conductors and liquid-vapor heat pipes. The tubes also appear to have the ability to function at very high temperatures, even up to the melting point of the materials used, and to support very high heat fluxes. Our tests to date support the high temperature capabilities in addition to the high thermal conductivities. However, the thermal conductivity is so high that accurately measuring the value is very difficult. We have therefore acquired nine 10' long Supertubes, 5/16" in diameter, and have set up a method for determining the thermal conductivity using high heat flux, a water cooled calorimeter, and a rake of over 30 carefully calibrated thermistors. This apparatus should provide an accurate means of determining the thermal conductivity, and will also allow us to check the high heat flux capability of the tube and to assess possible puzzling temperature distributions.

Figure 17 shows a data set in which the temperature across the length of a 10' long tube heated from the end and cooled in air is essentially constant, whereas a similar size copper tube would have the temperature distribution shown in the bottom curve. Increasing the thermal conductivity, k , of the copper by factors from 1000 to 30,000 shows agreement between the analysis and the data at 30,000 times that of the copper, although this is only a lower limit on the actual conductivity. Increasing the factor even more does not produce a discernible change in the curve relative to the data. We have also tried other methods to estimate the high thermal conductivities we have measured, such as the Ingenhous technique; these results also indicate very high thermal conductivities. However, we needed a more accurate means than previous tests with free convection cooled tubes with thermocouples, and therefore we devised the test apparatus shown in Figure 18.

The 10 ft Supertubes are heated by three 2kW coil heaters. Power for the heaters comes from a 3-phase 2 leg output power controller with two legs fused at 20 Amps. For safety reasons the power controller and fuses are placed in an enclosure along with a Wattnode[®] power

meter. A water calorimeter is used to measure the heat conducted along the Supertube. Fins, shown in Figure 19, are necessary to transfer the high heat flux to the water; these were fabricated in such a way that they can be easily attached to the Supertubes using hose clamps. Also, the fin design increases turbulence in the flow through the heat exchanger. Having the turbulent flow increases the heat transfer rate into the water, and also discourages boiling, which could occur with the high heat fluxes used.

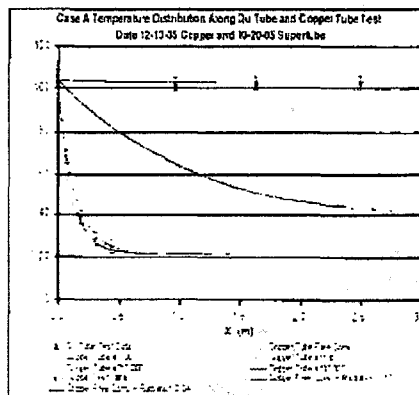


Figure 17. Comparison of Essentially Constant Supertube Temperature Distribution with Theoretical Distribution for a Standard Copper Tube and Rod, Showing that the Thermal Conductivity Must be at Least 30,000 Times that of Copper.



Figure 18. Experimental Apparatus for 10 ft Qu Supertubes.

Rocket Propulsion

The photo in Figure 27 is from the Society of Automotive Engineers book, *Advanced Engine Development at Pratt & Whitney: The Inside Story of Eight Special Projects 146-1971*, by Dick Mulready. Chapter 6 of this book, "Boost Glide and the XLR-129 – mach 20 at 200,000 Feet," mentions the McDonnell Douglas boost-glide strategic vehicle, as well as citing the key personnel at McDonnell Aircraft Company. Some time ago, a model showed up on the desk of a now-Boeing employee that was not readily identifiable. The author has an original model of this boot-glide strategic vehicle, and it matched the unidentified model shown in Figure 27.

The XLR-129 was a shuttle-class engine that operated with turbopump exit pressures of 3,500 psi. It was brought to full pressure operation for the U.S. Air Force in just over 3 months.¹⁴ In comparison, the space shuttle main engine (shown in Figure 28), operating with a lesser turbopump exit pressure, required 3 years to reach full pressure operation and never demonstrated reusability without overhaul.



Figure 27. Boost-Glide Strategic Vehicle With Pratt & Whitney XLR-129 Rocket Engine Installed, Circa 1964

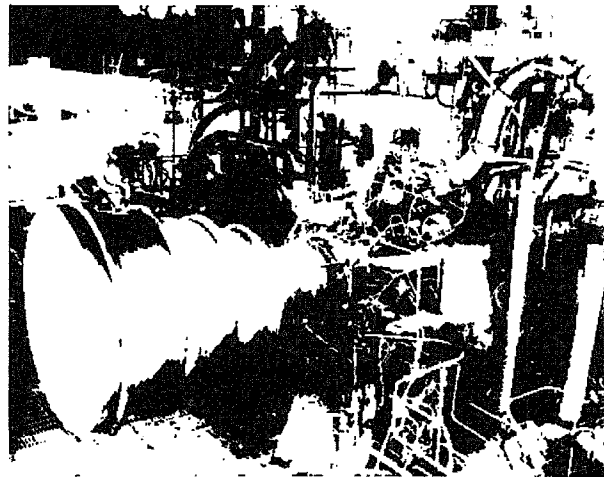


Figure 28. XLR-129, a Shuttle-Class Engine That Ran for 40 Test Cycles With Only Component Maintenance and No Engine Rebuilding

The final paragraph of chapter 6 in Mulready's book contains the following passage: "The liquid oxygen turbopump was the next component in line. However, before it was funded, NASA had started the space shuttle campaign, and the Air Force gave the XLR-129 program to NASA granting free use of the existing hardware to Pratt & Whitney. NASA promptly canceled the liquid oxygen turbopump because it would be unfair to our competitors to fund it." With the demise of the XLR-129, a rocket engine with a run record of 42 simulated flights (in the test chamber) without any overhaul disappeared. This engine was really the type of hardware a Kelly Johnston would oversee—that is, the best application of the industrial capabilities available in the skilled mechanics, engineers, and manufacturers. The only other engine of its class is the Russian RD-0120 engine manufactured by Autokinamatiki for the Energia launcher. This engine functioned on the test stand for 80 simulated flights to space and return before

overhaul was necessary. It, too, met its end in a government-terminated program, lost to future space launcher designers.

Two air-breathing rocket propulsion systems permit examination of a rocket-powered vehicle as an operationally viable commercial system with low-noise airport operation, reduced operational weight, and global deployability for a space-based FedEx or UPS (cargo is economically viable, passengers yet to be determined). The earliest of these is a rocket system that operates as an air-breathing rocket below mach 5.5. This concept dates to the late 1950s and the Marquardt Company. The termination of the first aerospace plane halted this work, but John Ahern¹⁵ continued his work, as did John Leingang¹⁶ at the U.S. Air Force Aero Propulsion Laboratory. Much of Leingang's work was kept out of the technical literature in the 1960s, so this is a current reference establishing that earlier work. John Ahern was one of the first analyzers of the Liquid Air Cycle Engine (LACE) concept, and one who identified the sources of irreversibility and approaches to minimize them. In Russia, Keldesh Institute independently began, conducting experiments with LACE systems, as reported at the 2002 conference sponsored by the Association Aéronautique et Astronautique de France and also by Rudakov^{17, 18} and Balepin.¹⁹ In Japan, NAL Mitsubishi and ISAS conducted experiments that were leading to an air-breathing rocket system, and an impressive, ice-free, 1-cubic-meter liquefying heat exchanger was demonstrated for the NASP visiting team in 1988.^{20, 21} With only one hydrogen test stand in Sendi, LACE development was deferred until the problems with the H-1 engine were solved. However, by then interest was lost. In India, research organizations used all of the published LACE documents to arrive at a credible system configuration and performance.²² Unfortunately, India at the time did not have the manufacturing skill and methods to make a functional LACE System.

There are two types of air-breathing rockets, both of which are based on using the recoverable energy in the liquid hydrogen to drive the systems, as diagrammed in Figure 29. In both systems, the liquid hydrogen absorbs the thermal energy in the inlet air stream to reduce the air temperature to nearly saturation in an upstream heat exchanger. In the LACE, as the name implies, a second heat exchanger liquefies the cold gas and a turbopump pressurizes the liquid air to the correct working pressure required by the rocket motor. The thermal energy is picked up by the hydrogen in cooling the gas, and the rocket (including the combustion chamber) is used to drive the expansion turbines powering the turbopumps (left sketch in Figure 29). In the Japanese system, a low-pressure ratio compressor pressurizes the cold gas before it enters into the downstream heat exchanger, increasing the quantity of liquid air produced per unit liquid hydrogen. With a heat exchanger in the rocket motor combustion chamber, there is sufficient thermal energy to power the expansion turbines compressing the saturated or liquid air and deeply cool or liquefy the incoming air to at least mach 5.5. In the deeply cooled system (Rudakov and Balepin), a turbocompressor compresses the cold gas to the injection pressure required by the rocket motor. The thermal energy picked up by the hydrogen in cooling the gas and the rocket (including the combustion chamber) is used to drive the expansion turbines powering the turbocompressor (right sketch in Figure 29). One of the difficulties with Bond's HOTOL (horizontal takeoff and landing) engine compared with Rudakov and Balepin was that HOTOL avoided the combustion heat exchanger at the expense of having the air-breathing rocket operate to less than mach 4, increasing the to-orbit weight ratio and gross weight and thereby making the concept less viable. In both

cases, the low-pressure hydrogen exiting the expansion turbines is entered into the rocket motor at a matching pressure.

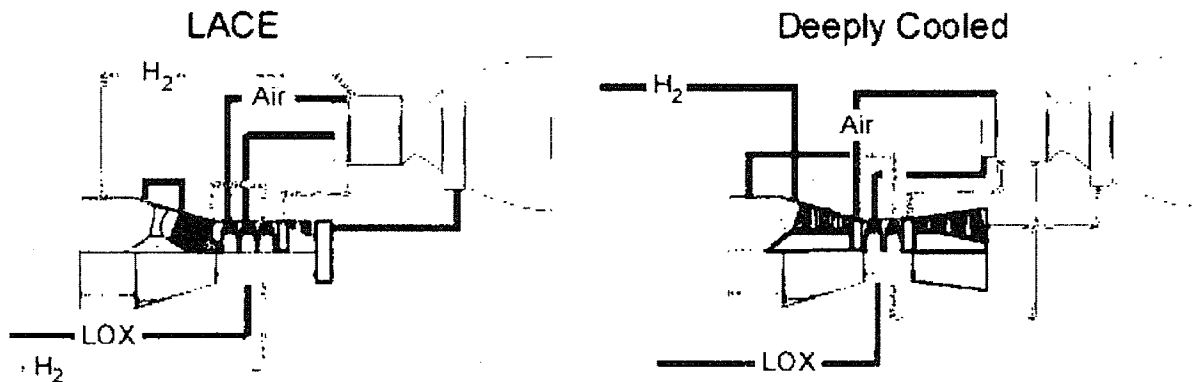


Figure 29. Two Rocket Air-Breathing Rocket Cycles to Mach 5.5. To the left is one employing liquefied air (LACE cycle). To the right is one employing high-pressure air cooled to near saturation.

There is always the option of direct ascent by rocket into a trajectory. Whether by turbojet or rocket, a million pounds of thrust is always noisy and smoke filled. We can thank the Russian design bureaus for arriving at a concept that eliminated the noisy, smoky, and hazardous launches by increasing the operational flexibility of the British HOTOL concept. Figure 30 shows the development of the all-rocket HOTOL system from the original HOTOL.²³ The original air-breathing rocket HOTOL, powered by the Rolls Royce 545 engine as developed by Alan Bond, essentially used all hydrogen fuel (except for space operations). The hydrogen required a volume about 5 times greater than a 6:1 LOX/hydrogen propellant for a rocket engine. The classical aerodynamicist's approach was to minimize drag and maximize the L/D ratio. But accelerating to orbital speed requires a low angle of attack and minimum drag coefficient at zero lift (C_{D0}), not maximum L/D ratio. The simple problem, recognized by Küchemann, was that the vehicle was too slender and therefore had a large wetted area compared with its reference planform area; hence, zero lift drag and structural weight were too high. Even when the BAE Systems team switched to an all-rocket and compromised the slenderness, this did not significantly reduce the wetted area. The Russian approach was to design a stout vehicle with a much lower ratio of wetter area to reference planform area.²⁴ The trapezoidal cross section of the FDL-7/Model 176 yields a ratio of wetted area to planform area less than the circular cross section of the

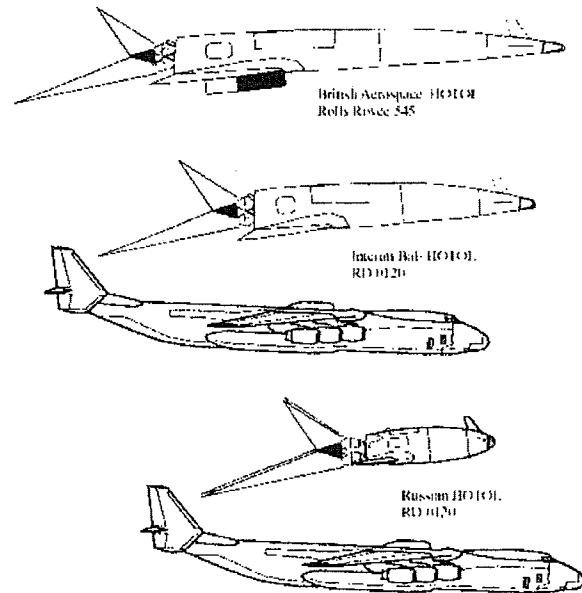


Figure 30. HOTOL Evolution: From Aerodynamic Optimum Configuration to Practical Launcher Configuration. The latter was developed through British Aerospace-Russian cooperation.

Russian HOTOL. However, NPO Molnyia provided a unique approach to space access by decoupling the attachment to a few fixed base operations and opening up space access to a global clientele, and not from a remote nation, but from Russia. NPO Molnyia's approach also removed the noise and smoke from a rocket launch to a mundane takeoff of a turbofan-powered transport.

The upper payload limit of the An-225 is 300 metric tons for the structural mounts on the top of the fuselage. With a conventional rocket, that limit was reached for the Russian HOTOL at 5.45 metric tons, not the 7 tons desired. With the addition of an air-breathing rocket to the initial part of the trajectory and the FDL-7/Model 176 configuration, that limit now is not reached with even an 11-ton payload.

The An-225 has the empennage modified from the An-124 single vertical and horizontal to an 'H' configuration. This permits the powered hypersonic glider to easily lift off the top of the vehicle, as the MBB Sanger wind tunnel test demonstrated. A second modified transport would be modified to carry the liquid hydrogen and liquid air to fuel the hypersonic vehicle, along with maintenance and support crew. The intent was to use the automatic launch checkout the author witnessed at Baikanour in 1988, wherein a Soyuz that arrived on its train carrier at 0500 hours launched carrying a Progress capsule at 1715 hours the same day. That should make a local launch possible within hours of arriving at the specified airport launch departure site. Again, we can thank the Russian design bureaus for arriving with a concept that might be the first economically viable global launch concept not tied to a fixed geographical launch site that employs robust, proven carrier aircraft.

As illustrated in Figure 31, a LACE system operating to mach 5.5 that has the same operational weight empty and 7-metric ton (15,435-lb) payload as an all-rocket reduces the liftoff gross weight of a HOTOL concept operating from atop a transport by 150 metric tons (330,000 lb). That enables a transport launch platform to carry an orbital launcher with a functional payload greater than 11 metric tons (24,225 lb). Payloads greater than 11 tons are determined by the size of the launcher atop the transport. The launcher can become too large for the transport to maintain stability and control. The exhaust temperature and therefore velocity of a LACE rocket are less than those of a hydrogen/oxygen rocket, resulting in a quieter launch and making launch from a transport more favorable. The LACE-powered vehicle is physically smaller than the rocket vehicle because the propellant weight and volume are less. The green line in Figure 31 is the propellant weight for the sized LACE orbital launcher. The important thing to remember is that the air-breathing rocket motor is the same as the all-rocket motor; only the propellant mix is different.

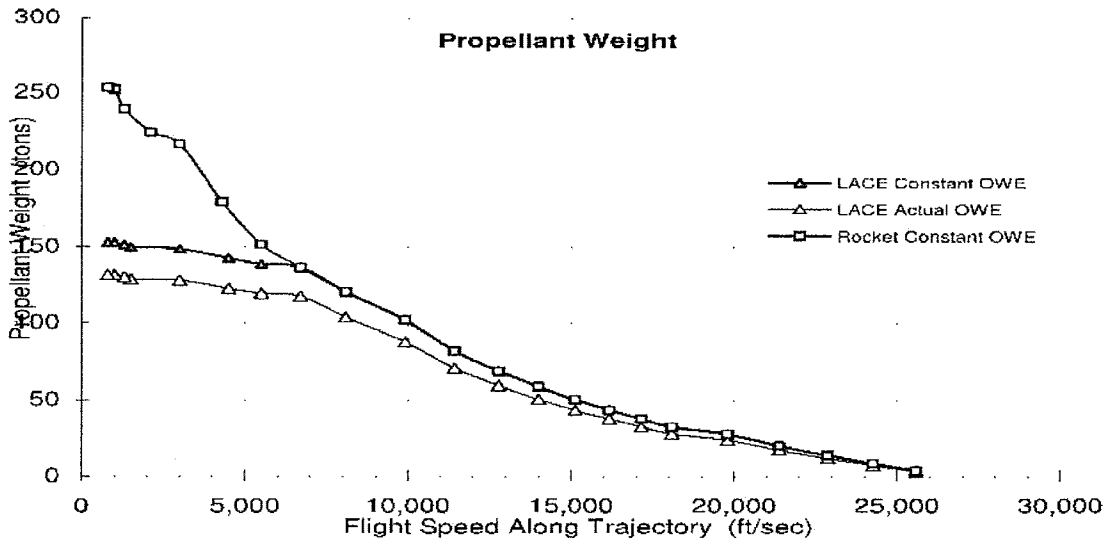


Figure 31. LACE Air-Breathing Rocket Reduces Gross Liftoff Weight by 150 Metric Tons and Uses Existing Rocket Engines

The LACE or deeply cooled cycle could also be adapted to operate in the FDL-7/Model 176 if it were a first stage to a two-stage-to-orbit system,²⁵ as shown in Figure 32 with a retractable, inward-turning inlet.²⁶ In this case, there is another version of the precooled air-breathing engine concept, called the KLIN cycle, that was invented by V. V. Balapin.²⁷ Like the LACE and deeply cooled systems, the KLIN cycle can significantly reduce the size and weight of a launcher. The KLIN™ Deeply Cooled Turbojet/Rocket Cycle incorporates a heat exchanger upstream of the compressor to thermally control the air to the compressor so a lower corrected speed of the compressor can be maintained with the increasing mach number. The cycle also thermally integrates an expander cycle rocket engine, one in which rejected thermal energy is used to drive the turbopumps and accessories. The initial cycle calculations have shown good results for hypersonic vehicle space launcher applications. For mach numbers less than mach 5.5, the turbojet and rocket operate as a single system providing the required total thrust for acceleration.

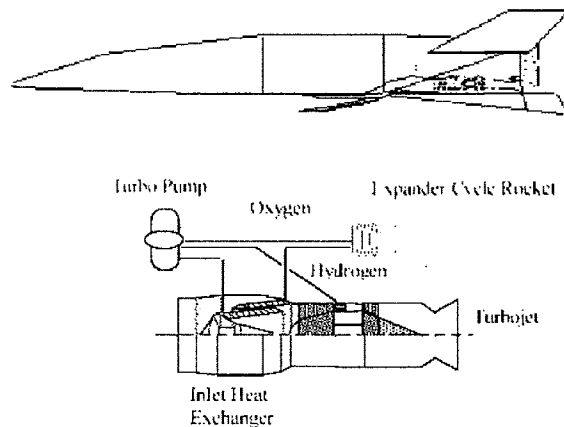


Figure 32. The FDL-7 Class of Vehicles With An Anthony DuPont Variable Capture and a Retractable Inlet Tested to Mach 5 Employing an Air-Breathing KLIN Cycle Rocket

Up-and-Down Operations

For an aircraft, the takeoff mode is not an issue: it is a runway takeoff and runway landing. However, for a space launcher, the issue is not so clear-cut. With mass ratios for launchers much greater than for aircraft (4 to 8, compared with less than 2 for aircraft), runway speed is impractical for some launchers with high mass ratios. The principal option is vertical takeoff, with horizontal landing remaining viable. The problem is that in some launcher studies, the study directives mandated horizontal takeoff regardless of the mass ratio. Many launcher studies have been thwarted by this a priori dictate of horizontal takeoff. Air-breathing propulsion is then stuck with a "too heavy" label because of the dictated takeoff mode. In reality, horizontal or vertical takeoff, like the configuration concept, is less a choice than a result of the propulsion concept selected. Horizontal takeoff requires that the wing loading be compatible with the lift coefficient the configuration can generate and the maximum takeoff speed limit.

Figure 33 shows results for highly swept delta planforms, such as that of the Model 176 and FDL-7. Takeoff speeds for blended bodies in the 200- to 230-knot ranges were postulated in the 1960s by using very large gimbaled rocket motors to rotate upward and cause the body to also rotate, lifting off the nose wheel as the vehicle lifts off with a thrust-supported takeoff. This concept was not known to have been implemented in an actual system. For space launchers, the takeoff speed of the basic delta is high (square symbols). If the takeoff speed is too high for the propulsion system chosen (because of the weight ratio), then the only way to decrease the takeoff speed is to increase the planform area for the system volume—that is, to reduce the Küchemann tau. This, unfortunately, introduces a cascade of incremental mass increases that result in an exponential rise of the takeoff gross weight (as shown in Figure 34). The only lift-increasing devices available are a leading-edge vortex flap or a retractable canard near the nose of the vehicle.

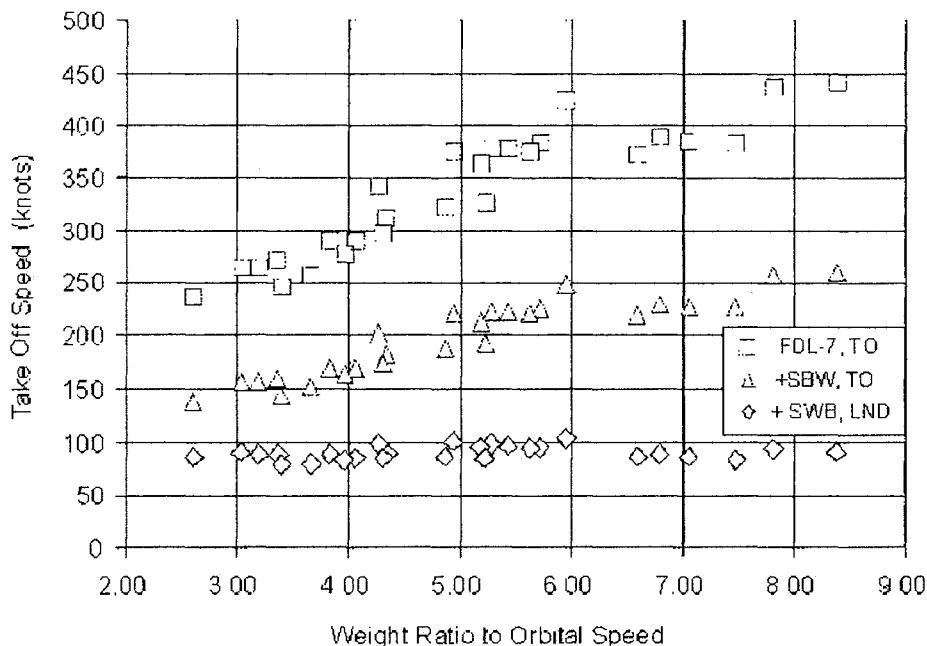


Figure 33. Takeoff and Landing Speeds of Minimum-Sized Launchers

Adding the switchblade wing (see inset photo in Figure 10) provides a reasonable takeoff speed for all mass ratios (green triangles). This takeoff speed with the switchblade wing deployed is approximately the landing speed with the wing stowed. With the wing deployed (blue diamonds), the landing speed is almost constant, since all of the launcher vehicles have very similar empty-plus-payload weights (operational weight empty). Then the landing speed becomes very modest, lower even than that of most commercial transports and military aircraft. With this approach, the switchblade wing can be either deployed or stowed, and the landing and takeoff speeds can be essentially equal, adding a degree of operational simplicity. The switchblade wing was designed with the expectation that the gliders would return with greater payloads than they delivered. Landing and takeoff speeds correspond to those of current military aircraft and commercial transports, at least for the lower mass ratios (5 or less). Whether the switchblade wing is deployed or stowed, a set of solutions exists in which the landing and takeoff speeds are similar.

Figure 34 begins with a solution map of vertical takeoff launchers, as represented by the shaded areas in the lower part of the figure. All of these data are for converged solutions, whereby the mission requirements are met and the mass and volume of each solution are converged. These solution areas represent the entire propulsion spectrum, from all-rocket (far right) to advanced air-breathing systems (far left). These solution areas are for vertical takeoff and horizontal landing (VTOHL), with a thrust-to-weight ratio at takeoff (TWTO) of 1.35 and a Küchemann tau equal to 0.2.

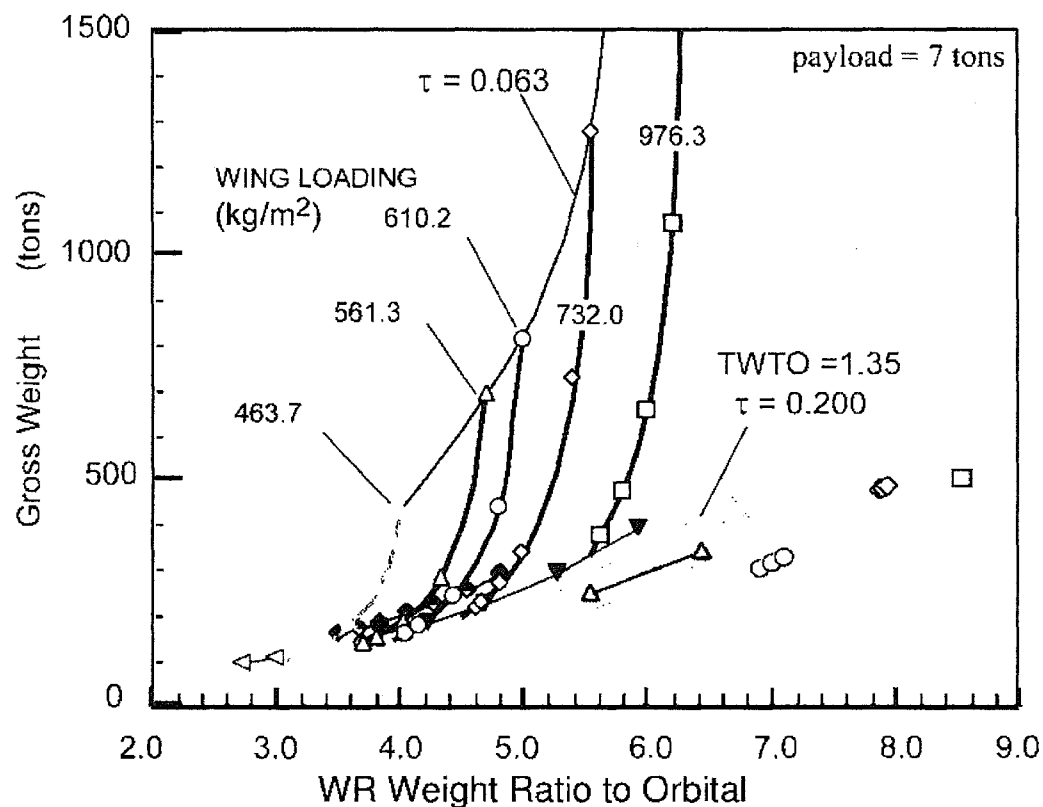


Figure 34. Horizontal Launch Not Practical Unless Weight Ratio is Less Than Four

Gross weight trends are shown for five different takeoff wing loadings for horizontal takeoff and landing (HTOL). Solutions for constant wing loading are shown for values of tau from 0.2 to 0.063. The curves sweep upward between tau = 0.2 and tau = 0.063 and are variable tau solutions for a fixed takeoff wing loading. The curve for 200 lb/ft² never converged at tau = 0.063 and is almost vertical. So if 185 knots is an acceptable takeoff speed, then the maximum weight ratio without significant weight penalty over vertical takeoff is about 5.6 (40 years ago, Dwight Taylor of McDonnell Aircraft determined the point to be a weight ratio of 5.5). This excludes conventional rockets but does permit high-performance air-breathing rockets and the KLIN cycle.

The point at which the VTOHL and HTOL modes have the same gross weight is then the maximum weight ratio for which there is no penalty for horizontal takeoff. For example, at a takeoff wing loading of 976 kg/m² (200 lb/ft²), the point at which the VTOHL and HTOL modes have the same gross weight is for a weight ratio of 5.5, or an air-breathing speed of mach 6 ± 0.3. For a takeoff wing loading of 610 kg/m² (125 lb/ft²), the VTOHL/HTOL boundary is now a weight ratio of 4.3, or an air-breathing mach 10.5 ± 0.5. This wing loading would be consistent with that of commercial transports and is also correct to air launch horizontal landing at about mach 0.72 and 35,000 feet. For a takeoff wing loading of 464 kg/m² (95 lb/ft²), the VTOHL/HTOL boundary is now a weight ratio of 3.4, or an air-breathing mach 13 ± 1.0.

For an air-breathing rocket, a mass ratio of 5.0 is achievable, resulting in a gross weight of about 230 tons. This is less than half the 480 tons for an all-rocket case. However, if a horizontal takeoff requirement is imposed a priori, the lowest wing loading for which a practical solution exists is 610.2 kg/m². At that point, the gross weight for the horizontal takeoff solution is about 800 tons, almost twice the all-rocket value. If a study team is not aware of the comparison to vertical takeoff, it may draw the improper conclusion that the propulsion system caused the divergent solution. For lower wing loading, the solution curve becomes vertical, and the solution will not converge. The conclusion is that if the weight ratio is greater than 4.3, the best vehicle configuration is vertical takeoff or an air-launched configuration (all of the vehicles have a horizontal landing mode). If the goals are the lowest gross weight and the smallest sized vehicle, then it is important to let the characteristics of the converged solution themselves determine the takeoff and landing modes. To translate the takeoff wing loading into takeoff speed and the landing wing loading (operational weight empty plus 10-percent margin, so the launcher can return with payload and fuel residuals onboard), use legacy correlations from McDonnell Advanced Engineering. The equations for landing and takeoff speeds are given below:

$$\begin{aligned} (V_{TO})_{\text{knots}} &= \sqrt{227.114 \cdot LTO} \\ (V_{LD})_{\text{knots}} &= \sqrt{173.675 \cdot LLD} = \sqrt{173.675 \cdot \frac{LTO}{WR}} \end{aligned} \quad (4)$$

As pointed out previously, an a priori selection of horizontal takeoff (HTO) can have a very deleterious effect on the weight and size of an SSTO launcher. For example, a VTOHL air-breather propulsion concept should have a gross weight of 300 to 325 metric tons at takeoff, compared with 750 tons for an all-rocket VTOHL propulsion concept. A

forced HTO mode would instead have a gross weight in excess of 1,000 tons. So the resulting observation was "See! Air breathers are not lighter than all-rocket!" And so the rocket proponents have defeated an air-breathing solution since the first aerospace plane in 1958.

Launch Options

Previously, an option was presented for a mobile launch platform that was limited to an 11- to 12-metric ton (24,225- to 26,460-lb) payload. This section presents a conventional vertical launch site that provides for frequent, scheduled launches and no intrinsic payload weight. In a discussion with the author, Lozino-Lozinski questioned the practicality of the NASP, describing it as nothing more than a very large orbital-entry-protected propellant tank. His approach was to minimize the volume of propellant tanks that required orbital-entry protection. Prior to meeting DARPA's Robert Williams, the MDC had the same philosophy, as shown in Figure 35.

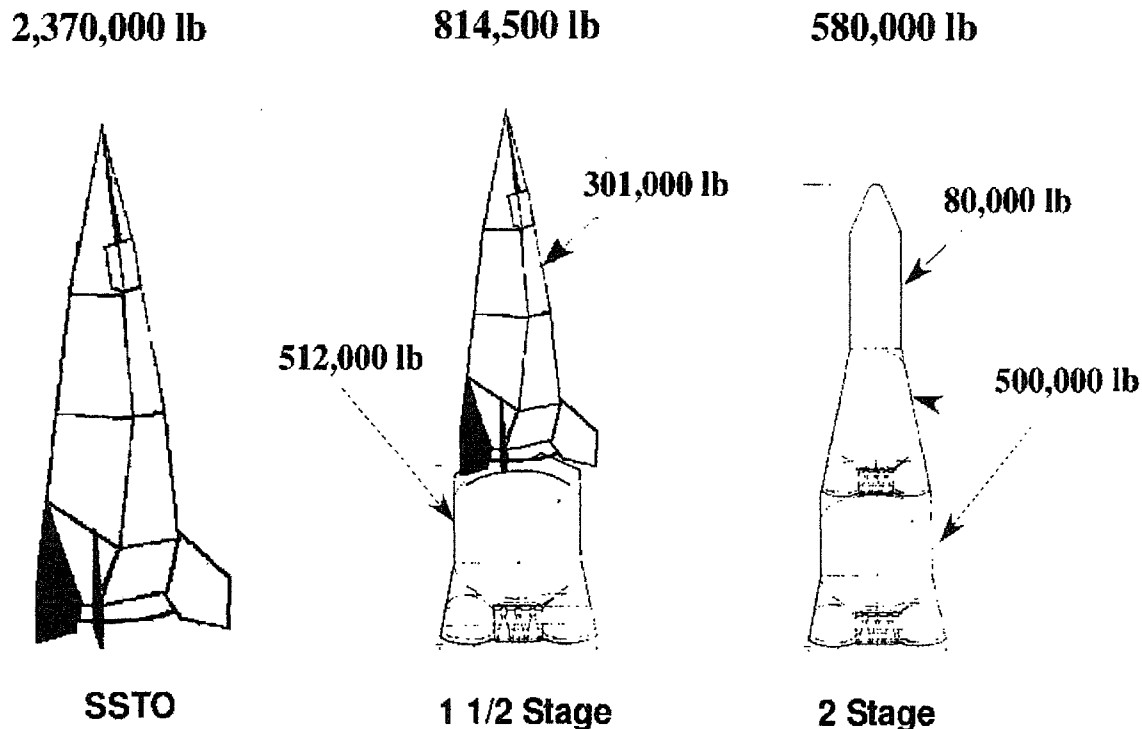


Figure 35. Propellant Tanks That Are Not Reentry Vehicles Greatly Reduce System Weight. Venture star orbital maneuver rules.

This was the MDC manned aerospace vehicle approach we briefed before the NASP. The size, thermal protection system surface area, and weight of the SSTO vehicle to just a stage-and-a-half concept is significant. All of the booster segments were fully recoverable and reusable with rebuilding. The cargo capsule was not recoverable. This operational concept envisioned frequent, scheduled launches at least equal in number to those of the 1964 MOL support launcher—that is, 100 to 150 launches a year.

As per the U.S. Air Force requirements we were working with, these TAV were piloted and therefore had retractable crew stations that could provide forward visibility when permitted by thermal conditions. The launch system (see Figure 36) was adopted from the U.S. Air Force Thor IRBM launch system and from observations when the author was at Baikanour, Kazakhstan. The vehicles were in dry horizontal storage and were serviced and loaded horizontally. The hanger/shelter was rolled back for erection to vertical position and then fueled. The launch sequence was patterned after the Baikanour Soyuz launch, which is 12 hours. The Thor IRBM launch sequence (LOX/RP-1) was 15 to 18 minutes. As in Baikanour, the payloads are not to be loaded into the vehicle and then remain there for weeks before checking out. What is loaded into the vehicle are checked-out payloads that need only to be attached to the carrying hardware. At Baikanour there were about seven pre-checked out Soyuz and Progress payloads in plastic wrap inerted with argon. The goal was to be able to launch a Soyuz launcher within 7 to 12 hours in the event of an orbital emergency. The Soyuz launchers were in dry storage and brought in on a railcar.

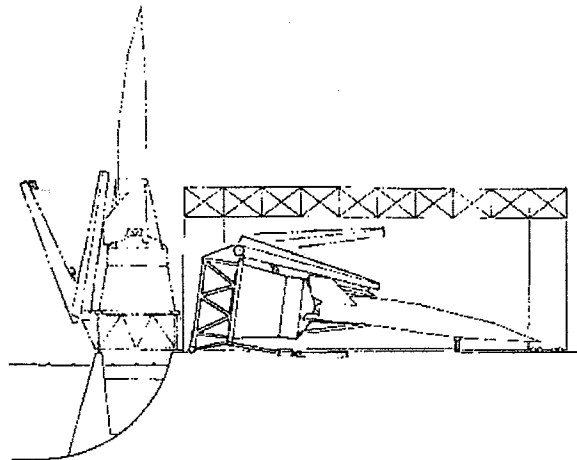


Figure 36. Simple Horizontal Integration and Vertical Launch Provides Rapid Launch Capability

With the Russian fully automatic checkout and fueling approach, this would certainly be possible. Figure 37 shows an artist's illustration of a TAV launch and recovery operational base. The boosters are a concept from Joe Thurgau of MDC Huntington Beach "Toss-Back" boosters that, after separation, rotate 180 degrees and fire their rocket motors to "toss back" to the launch site. An infrared guidance system steers the booster to a recover lake for a powered vertical landing (upper righthand portion of the illustration). The booster rocket engines are nongimbaled, sealed with the heat shield base. Either the 1-½ stage or the 2-stage systems could be launched. It would have even been possible to launch a booster by itself to rapidly transport it to another launch site (lower center portion of the illustration). Runways are provided for returning hypersonic gliders (upper center portion of the illustration), as well as for service and supply aircraft. Housing, maintenance facilities, and other buildings are on adjacent property. It certainly would be possible to launch this system from Vandenberg Air Force Base or Cape Canaveral,

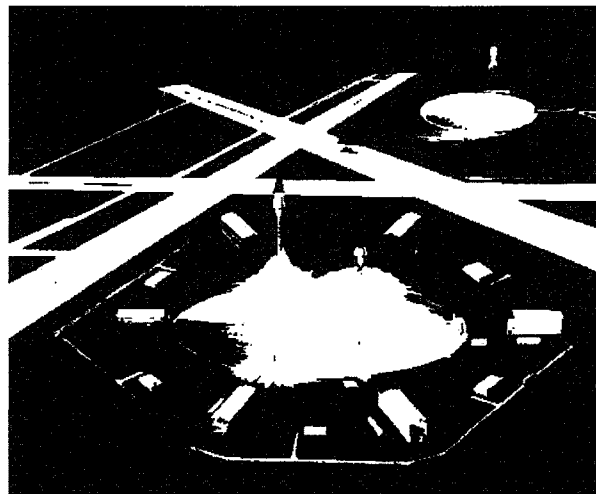


Figure 37. A Vertical Launch Complex Provides Vertical Toss Back Booster Recovery and Horizontal Landing Facilities for the Hypersonic Gliders

but we believed new launch complexes would be required to achieve the desired launch rates and to accommodate sustained-use vehicles.

This all seems impossible given today's launch operations and preparation time, but in 1964 it was considered possible both in the United States and in the former Soviet Union. It appears that two known companies proposed on the MOL support system, as shown in Figure 38. The Model 176 preliminary launches were to be on a Martin Titan IIIC. This was adequate for testing, but the minimum launches for one year of support of MOL was 74 launches. That 74 Titan IIICs could achieve a sustained manufacturing rate or a sustained launch rate was not considered. So both Lockheed Aircraft and McDonnell Douglas proposed a self-sustained operational system using recoverable lateral propellant tanks. There were no engines on the lateral tanks as there were in the aircraft since they were simply drop tanks.

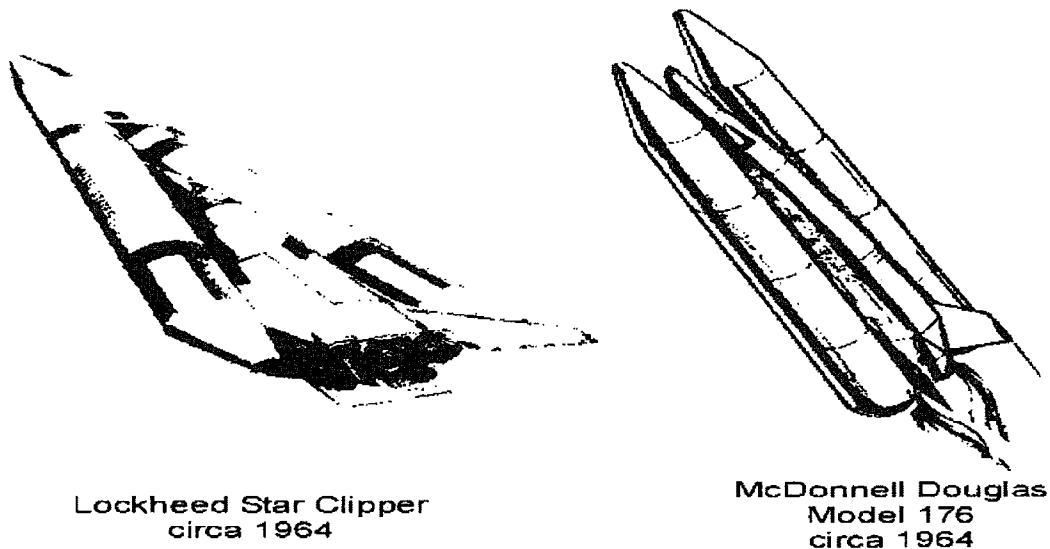


Figure 38. A 1964 MDC Astronautics, St. Louis, Briefing Defined a MOL Support System With 10 Launchers That Could Fly 100 Missions a Year for 15 Years. Lockheed Aircraft and McDonnell Douglas both had candidates.

Atmospheric Variations

The published approach to determining glide range is to assume the global atmosphere definition is a series of concentric, constant-density shells. The 1962 standard atmosphere follows the 1959 standard atmosphere and previous standards. NAVAIR-5-1C-59, Harold Crutchner,²⁸ details the Northern Hemisphere by month for every 10 degrees of longitude from 1931 to 1964. According to Crutchner, these atmosphere descriptions were not intended to be engineering atmospheres but to be standards to ensure that aircraft flying globally would have adequate altitude clearance. The 1962 atmosphere represents the average of all daily reports by the worldwide reporting stations between +30 and +60 degrees latitude for the spring and fall equinox minus one month to plus one month represented as a +45 degree average atmosphere.

Figure 39 shows the deviation from the 1962 standard atmosphere for a hypersonic glider entering the atmosphere from the central South Pacific (summer) to northeastern Russia (winter). The deviations from constant-density shells based on the 1962 standard atmosphere are significant. With today's computers, not ignoring the actual atmosphere is only a bookkeeping task. Hypersonic glide ranges at near maximum L/D ratio are to be generated. The local density is critically important, as it is determined by the lift coefficient for L/D maximum.

$$q = \frac{W/S_{plan}}{(C_L)_{max L/D}} g \left[1 - \left(\frac{V}{25,535} \right)^2 \right] = 1188.5 g \left(\frac{V}{1000} \right)^2 g \sigma \quad (5)$$

The seasonal variations are enough that the glider should have the correct density and temperature distribution in its flight-control computer so that unexpected alterations in the flight trajectory are not mandated during entry. The atmosphere is analogous to a constant-energy system—if the lower altitudes are hotter, the upper altitudes are colder, and vice versa.

In terms of deviations from the standard, the coldest upper-altitude temperatures most likely encountered are at 50,000 feet over Saudi Arabia in summer, and the warmest atmospheric temperatures are at 27,000 feet over Russia in winter.

1962 Standard Atmosphere
 1966 Standard Atmosphere Supplement
 1959 Selected Meridional Cross sections of the Northern Hemisphere NAVAIR-50-1C-59

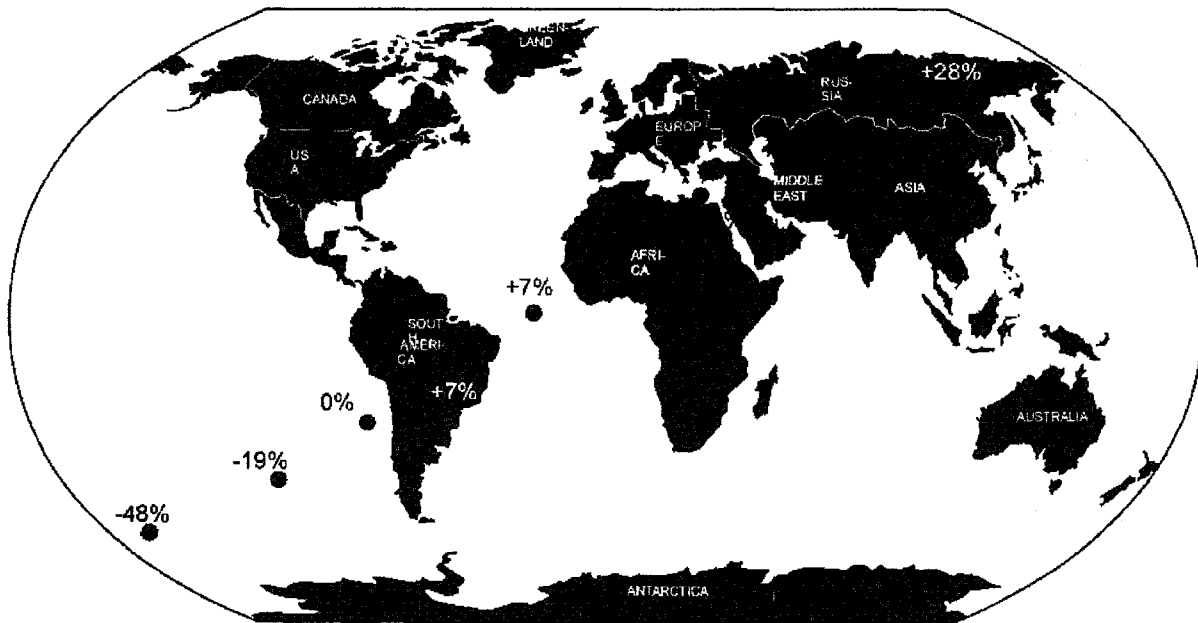


Figure 39. Earth's Atmosphere. Earth's atmosphere is not a series of concentric, constant-density shells or globally uniform, and flying from one hemisphere to another entails significant deviations from standard definitions.

Conclusion

The AFFDL fabricated a half-scale mockup of the stage and one-half Model 176 configuration³⁰ shown in Figure 40. The strap-on tanks provided propellants to about mach 6 or 7, after which the mission continued on internal propellants. Note the windshields installed in this 1960s mockup. This was a two-to-four-person military experimental vehicle to prove out the concept. The FDL-7 was identical to the FDL-5 except for the control surfaces. The FDL-5 had a single central vertical and fixed horizontal control surfaces with trailing-edge flaps. The FDL-7 discarded the single vertical and used the all-flying "V" verticals shown in Figures 10 and 12. The FDL-5 would have encountered stability and control issues had schedules and resource availability not forced the earlier configuration as the mockup. This was a vertical-launch, horizontal-landing configuration that had all the elements a full-scale operational vehicle would have (see Figure 38). In a very short time, however, the path the United States took to space changed, and most of this work was abandoned and discarded.



Figure 40. FDL-5 Scale Model of a Stage and One-Half Depicted²⁹

One of the key elements of the McDonnell Douglas TAV concept was a detachable nose section that was itself a stable hypersonic glider, as shown in Figure 41. The escape craft did not have the performance of the full-scale vehicle, but it could exceed the glide capability of the current space shuttle. Like the basic glider, the escape craft was automatically separated from the glider until the crew could establish landing site coordinates and a glide trajectory. The escape craft had the same operational envelope as the operational glider, so the crew always had the potential for a safe escape from a damaged or failing operational vehicle.

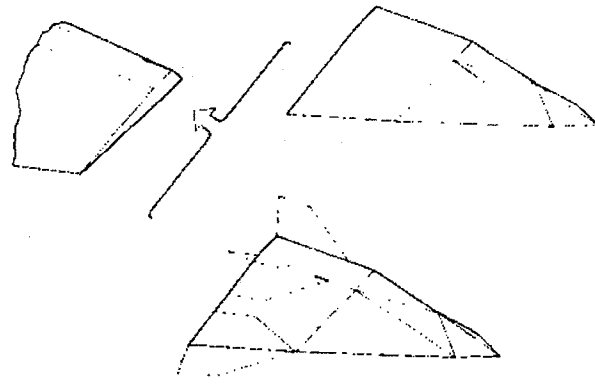
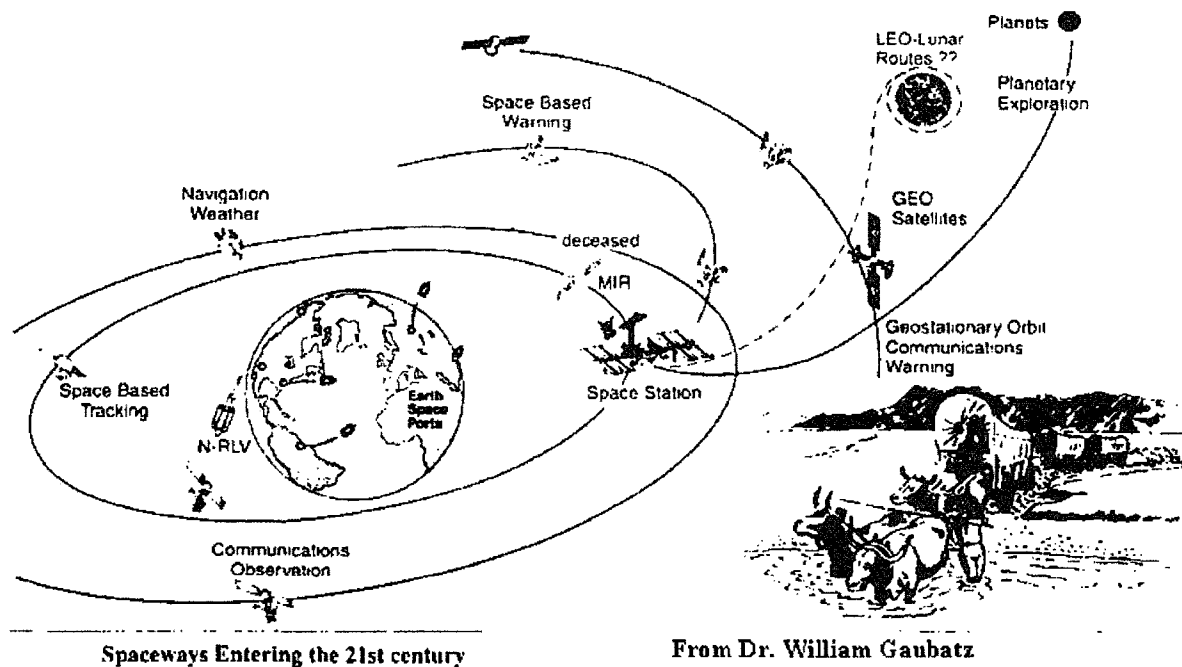


Figure 41. The FDL-7 and Model 176 Class of Hypersonic Gliders. The FDL-7 and Model 176 class of hypersonic gliders had integral, stable, controllable hypersonic-capable escape craft.

A common misconception is that a hypersonic glider's turn radius is so large that a hypersonic turn is of no practical operational use; that is not the case. Figure 42 shows nominal mach 15 and mach 10 turns initiated at Edwards Air Force base. This chart, from the NASP press kit release, shows two flight-test paths over North America initiating a 2g turn. For the 1968 McDonnell Aircraft HyFAC study,³¹ the landing turn



Spaceways Entering the 21st century

From Dr. William Gaubatz

Figure 43. Where We Are Today

Although not addressed in the frontline technical or popular press, a critical element in reaching space beyond Earth is the establishment of a space infrastructure around Earth and the moon. The concept of this infrastructure as a train marshalling and switching yard is appropriate. The rail control center serves as a center of operations for switching, long-haul train assembly, transfer of goods, and refueling and repair of space assets. Likewise, the orbital stations serve as centers for switching payloads between carriers and the required orbit, long-haul space exploration vehicle assembly, transfer of goods to human habitats and manufacturing facilities, and return, refueling, and repair coordination. This is no trivial activity and will take a commitment as dedicated as the Apollo program to achieve.

Without an infrastructure, we are doomed to expendable vehicles at low launch rates for specific, one-time missions with no semblance of an infrastructure. Neither the United Kingdom nor the United States had any long-distance, two-way commerce until the railroads were established. After that, cities and commerce centers were created, enabling two-way commerce. The space business has it backwards: There is no commerce until the infrastructure is in place, not vice versa.

How are we ever going to get here? How are we going to create a LEO infrastructure that can support the LEO, geostationary orbit, and lunar assets depicted in Figure 44? Is it a technology issue? Hardly! We have known for 50 years how to create it. Werner von Braun had Walt Disney create a clear visual image of what is required. But nobody listened, as we were too busy creating new things and throwing away the old things, destroying any development continuity. A good example is the destruction of the capability to make Saturn I and Saturn V launchers.

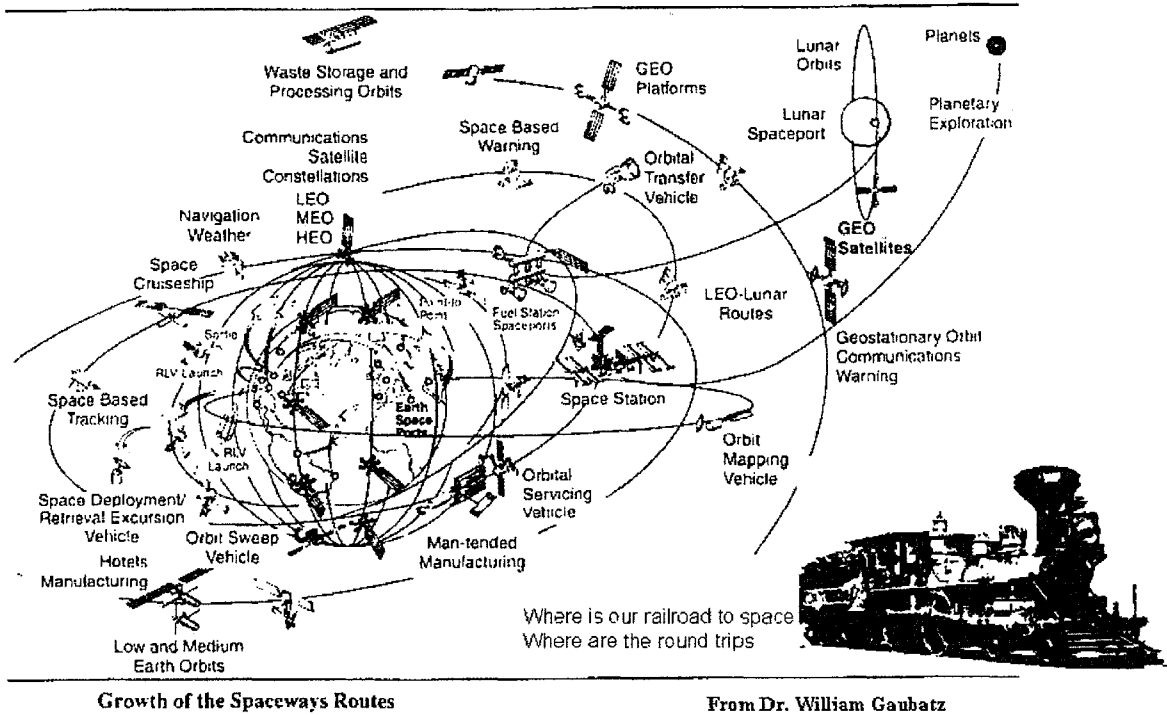


Figure 44. Where We Could Be If We Can Recapture the Engineering Confidence and Expertise of the Apollo/Saturn V Era

What is not shown in Figure 44³² is a solar power station that beams power to the Earth's surface or space assets or a power station warehouse that provides hardware for the power satellites in geostationary orbit. Whether a solar power satellite has the energy conversion efficiency to provide affordable energy to Earth or space assets comparable to what nuclear power stations could provide remains to be seen. Reports by H. H. Koelle of the University of Berlin provide excellent information on solar power stations.³³ In fact, the singular reliance on solar cell electric generation may doom all power stations until a more efficient and durable conversion system is identified. As with any thermodynamic generation system, the rejected heat becomes a major issue. As the Long Duration Exposure Facility materials evaluation satellite proved, space is a very hostile environment, and we have yet to identify slowly or nondeteriorating materials and construction concepts. Nicholi Anfimov, in a private communication, stated that the hub of the MIR orbital station (15 years in space) was so riddled with solar particles that it was beginning to leak, even though there were no visible holes. The complexity and extent of the space infrastructure are such that a significant commitment of human and monetary resources will be necessary if this infrastructure is to advance beyond a solitary orbital station with limited capabilities.

Figure 44 identifies the elements necessary to build the infrastructure but does not address the assets required to establish and sustain that infrastructure. Table 2 lists systems and functions of the infrastructure shown in Figure 44. Future global space is a crowded and busy place.

Table 2. Elements of the Space Infrastructure Shown in Figure 44

	Orbital System	Function	Orbit
1	Sustained Use Launcher	High frequency, modest payloads	LEO/MEO
2	Expendable Launcher	Low frequency, heavy payloads	LEO
3	Point-to-Point Transfer	Points on Earth or orbit	
4	Operations Center/Space Station	Operations Coordination/Research	LEO/MEO
5	Orbital Servicing Vehicle	Maintains in-orbit vehicles	All
6	Fuel Station Spaceport	Refuels orbital vehicles	LEO
7	Spacebased Manufacturing	Human based low "g" manufacturing	LEO
8	Man-Tended Manufacturing	Robot based micro "g" manufacturing	LEO/GEO
9	Orbital Sweep Vehicle	Orbital clean-up vehicle	All
10	Waste Storage and Processing Vehicles	Processes & disposes human and manufacturing wastes	HEO
11	Navigation/Weather	Supports travel network	LEO/MEO
12	Orbital Mapping Vehicle	Measures resources & geography	LEO/MEO
13	Space Based Warning	Military and Asteroid warning	HEO/GEO
14	Spacebased Hotel	Space tourist facilities	LEO/MO
15	SpaceCruiser vehicle	Human Transport and Rescue	LEO
16	Communication Satellite Constellations	Supports telecommunication systems	All
17	Orbital Transfer Vehicle	Orbital Altitude/Plane Change	All

UNCLASSIFIED//~~FOR OFFICIAL USE ONLY~~

18	LEO-Lunar Vehicle	Transport to Moon & return	LEO
19	Space Deployment Retrieval Vehicle	Recovers spent vehicles Replaces spent vehicles	All
20	Space Excursion Vehicle	Placement of new systems	LEO
21	GEO Platforms/Satellites	micro "g" and magnetic field space	GEO
22	GEO Communications and Warning Vehicles	Fixed Equatorial Position	GEO
23	Lunar Spaceport System	Lunar transportation/research hub	Lunar
24	Lunar Orbital Vehicles	Support Lunar activities	Lunar
25	Planetary Exploration Vehicles	Near & Deep space vehicles	LEO/Lunar

Appendix A: Historical Perspective

The four reports listed below and summarized in this paper are as applicable today as they were when they were released in 1964 and 1965:

- Robert R. Stephens; "Mission Requirements of Lifting Systems-Engineering Aspects"; Volume I Condensed Summary; McDonnell Aircraft Company Report B831 for NASA Manned Spacecraft Center; contract NAS-9-3562; August 1965.
- Robert R. Stephens; "Mission Requirements of Lifting Systems-Engineering Aspects"; Volume II Mission Analysis – Spacecraft Selection – Performance Analysis; McDonnell Aircraft Company Report B831 for NASA Manned Spacecraft Center; contract NAS-9-3562; August 1965.
- Robert R. Stephens; "Study of the Engineering Aspects, Mission Requirements of Lifting Systems"; Summary of Significant Results and Figures from Report MAC-B831; McDonnell Aircraft Company Report B947 for NASA Manned Spacecraft Center; contract NAS-9-3562; August 1965.
- "Manned Hypersonic Test Vehicle Study"; McDonnell Aircraft Company Report A9727 for United States Force; contract AF(33)600-2751; August 1964.

These reports describe an operational space station with an operational spacecraft fleet to support the orbital station in space. The term operational is used because the concept was not for a research and development spacecraft like an X-15 but a transportation system that moved resources to and from space, much like an operational FedEx or UPS operation. The work in the mid 1960s by a number of aerospace companies set the stage for the discussion of the development of the spacecraft configurations based on requirements and the propulsion systems that emerge to meet those requirements. These four reports are representative of the approach and designs that were prevalent in that period. Those involved with developing the orbital station and its supporting fleets of operational spacecraft were fully convinced that the industrial capability, materials, and resources permitted successful accomplishment of the task in 1962. The space station goals and the spacecraft required to meet those goals are especially interesting in light of today's discussion about crew rescue vehicles and the crew complement that should staff the International Space Station. What is different was that the station was a rotating station to provide a fraction of the Earth's gravity and was fabricated primarily from empty Saturn rocket components sent to orbit that were fitted with provisions to make them habitable.

The purpose of the study was to establish the operational requirements, spacecraft configuration, and requirements. The principal support mission was designed around a rotating space station constructed from Saturn 1B components and Saturn 1B lifted components. The station was designed for 20 to 27 persons, each on the station for a 6-month period. The nominal life of a given research program was assumed to be as long as 5 years. The spacecraft that supported the orbital station would be designed to carry 9 to 12 persons or materials to resupply the station. For that goal, a 7-metric ton payload (15,435 lb) was deemed sufficient. The study identified that each replacement person would have a 994-lb (450-kg) resource supply payload to accompany each crewmember. For a 12-person crew-replacement mission, the crew-replacement

payload would be 15,228 lb—well within the payload capacity. The operating parameters for the station were a nominal 21-person crew with provisions for up to 27. This study determined that 47,000 lb (21,315 kg) of resources were required per crewmember per year. So for 1 year and a 21-person complement, 448 metric tons of supplies would need to be lifted to the station for crew support, not counting propellants to maintain the station orbit. With 21 crewmembers, 4 flights per year would be required to meet the 6-month assignment requirement. To lift the crew supplies to the station would require 64 flights per year, not counting propellant- and hardware-replacement missions, which might require another 5 to 6 flights per year. The minimum number of flights to a large station would be 74 flights per year. From a military mission analysis, that would require a fleet of 10 aircraft (without operational spares) flying 7 times a year for 15 years and a 100-flight operational life. The spacecraft and systems considered in the study were:

- Ballistic, derivative Apollo capsule, Rockwell.
- HL-10 lifting body, NASA Langley.
- Wing body, X-20 derivative, Boeing.
- Variable-geometry lifting body, Model 176, McDonnell Douglas.
- Operations and logistics requirements, Lockheed, NAS-9-1422.
- Manned Orbiting Laboratory (MOL), Lockheed, NAS-9-1688.
- Manned Orbiting Research Laboratory (MORL), McDonnell Douglas, NAS-1-362.

This summary report contained a large number of recommendations and conclusions. Those that were pertinent to the Saturn 1B and Saturn V rocket launchers and the rotating space station are not listed. Only those related to the vehicle and propulsion system are given.

- Among the lifting-body spacecraft, the variable-geometry spacecraft provides the best combination of hypersonic maneuvering and landing performance.
- A 9- to 12-passenger payload with equipment is recommended.
- An abort system for both low-altitude and high-altitude abort and escape is required.
- Structural concepts and materials applicable to the loads and heating of lifting spacecraft are within the present (that is, 1965) state of the art.
- The weight factor for lifting spacecraft results primarily from a larger surface area and only secondarily from the associated spacecraft environment.
- Radiation-cooled structures are generally lighter than other structural concepts.
- For surface temperatures above 2,200 °F (1,204 °C), refractory metals are required, and coating life is the major refractory metal limitation (applies to carbon-carbon today).

- Meteoroid penetration or spalling of the thin refractory metal shingles may be a problem during a 180-day stay on orbital storage as a rescue vehicle, and some form of protection may be required.
- A readily refurbishable and repairable heat-protection system consisting of a water-cooled inner body, insulation, and a radiation-cooled external surface is recommended.

The goal was to build a test vehicle that initially would achieve at least mach 6.5 at 100,000 feet (30,480 meters) for at least 5 minutes test time. As scramjets became available, that would be extended to higher mach numbers and altitudes. As part of the spacecraft definition study, four fuels were considered: hydrogen, kerosene (JP-5), methane, and propane. The propulsion systems considered were:

- Turbojet-ramjet/scramjet.
- Integrated turboramjet.
- Rocket-ramjet/scramjet.
- Carrier aircraft/vehicle with ramjet/scramjet spacecraft.

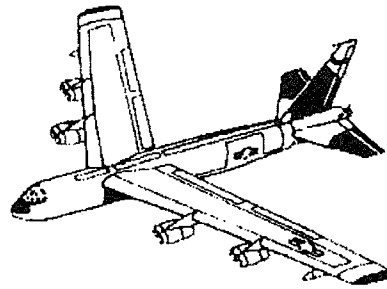
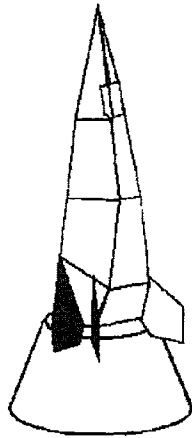
The closest study to respond to these findings was the NASA-sponsored HyFAC studies executed by McDonnell Aircraft Company of the McDonnell Douglas Corporation.³⁴

Appendix B: Aeropropulsion Integrated Vehicle

A launcher that uses air-breathing propulsion in a portion of its flight to exit the atmosphere has the same entry issues as the rocket-boosted hypersonic glider. However, the capture of atmospheric air to create thrust by chemical combustion is a different issue, as it configures the underside (aerodynamic compression side) as a propulsion system that produces more thrust than drag and also produces lift. For the propulsion system to function efficiently, the dynamic pressure and air mass flow per unit area must be higher than a rocket exit trajectory, as it is the airflow mass that enables the propulsion system to produce thrust in excess of drag so the vehicle can accelerate. So in this case we have a propulsion-configured vehicle. Neither the shape of the vehicle nor the trajectory it flies is arbitrary. The air breather does not exit the atmosphere as quickly as the rocket but stays in the atmosphere to the point where the transition to rocket propulsion occurs—usually set when the air-breather propellant per unit change in velocity is equal to or greater than the rocket propulsion, usually at about mach 12 to 14. The air-breathing propulsion system mechanical, aerodynamic, and thermal loads act longer and are of greater magnitude than the rocket-powered vehicle. In fact, the dynamic pressure—that is, the pressure of the air impacting the vehicle—is about 10 times greater than the entry dynamic pressure of the hypersonic glider. In this case the principal thermal load is encountered during exit from the atmosphere and the vehicle must be configured to generate sufficient thrust to provide a strong acceleration. So an air-breather configuration is different from the hypersonic glider, because the hypersonic glider has not been configured to fly extensively in the atmosphere and produce thrust from captured airflow. Like the hypersonic glider, this vehicle needs the same glide performance at entry. However, with the thermal protection designed by the high exit loads, the entry design is one of detail in maintaining stability and control and of achieving a comparable glide L/D ratio. The carried oxidizer is heavy and requires more engine thrust to lift it into space. A hydrogen/oxygen rocket, vertical-launch vehicle with a 7,000-kg payload has a gross weight in the 450,000- to 500,000-kg range and a 50,000-kg operational weight empty (that is, with the payload loaded). The engine thrust for a vertical takeoff is about 607,000 to 820,000 kg. A modest-performance combined-cycle air breather with a 7,000-kg payload and a 50,000-kg operational weight empty has a gross weight in the 200,000- to 225,000-kg range. The engine thrust for a vertical takeoff is about 270,000 to 304,000 kg. Most of the gross weight reduction is from the lesser amount of oxidizer carried and the lighter propulsion system weight.

Appendix C: TAV Operational Costs

Art Robinson was the deputy program manager for the MDC Manned Aerospace Vehicle Group at MDC Astronautics, Huntington Beach. Working with Art, the St. Louis part of the team prepared a work breakdown structure for servicing and maintaining an Air Force transatmospheric vehicle (TAV) based on a B-52 squadron. Larry Fogel of Decision Sciences visited several B-52 bases and discussed the operational concept and repair/maintenance work structure with the B-52 crews and maintenance personnel. The result was an estimate of the costs for operating a squadron of TAVs that had the same flight frequency as the B-52 squadron. The result for the one-and-a-half-stage TAV is shown in Figure 45. As might be expected, orbital operations are substantially more costly than atmospheric operations (aerodynamic cruise of hypersonic long-range glide). With an operational range greater than a refueled B-52, the TAV has a lower cost than the once-refueled B-52. The orbital cannot be compared directly with a B-52 since in achieving orbit the TAV has essentially infinite cruise range and duration limited only by the crew. The concept of operations was essentially that shown in Figure 37 installed on a U.S. Air Force SAC base. Although the SAC flight crews concentrated on potential nuclear missions, the presentation focused on a wide spectrum of kinetic penetrators installed in a rocket-accelerated entry nose cone. The terminal speed of the entry nose cone was in the 12,000 to 14,000 feet/second range. At that speed the energy delivered per unit weight was much greater than a spherical charge of HBX-6 because the kinetic energy was directly delivered to the target. The weapons spectrum could address a very wide range of targets that could be disabled or made nonfunctional or be destroyed with minimal collateral damage.



Cost \$97,000,000 Atmospheric Cruise
\$251,000,000 Orbital

Cost \$71,000,000 B-52 only*
\$140,000,000 Refueled B-52

*annual costs per DAA (14 vehicles)

Larry Fogel
Decision Sciences
Titan Corporation
Spring 1984

Figure 45. McDonnell Douglas Astronautics (Huntington Beach)-Funded Study of TAV Operational Costs

Appendix D: Landing Ellipses for Hypersonic Gliders

Figure 14 graphically shows the cross (lateral) range and down range for various hypersonic gliders. The lateral range and down range describe a landing ellipse for a vehicle entering the glide at 22,400 feet/second as shown in Figure 46. The 0,0 point is the beginning of the entry or glide trajectory.

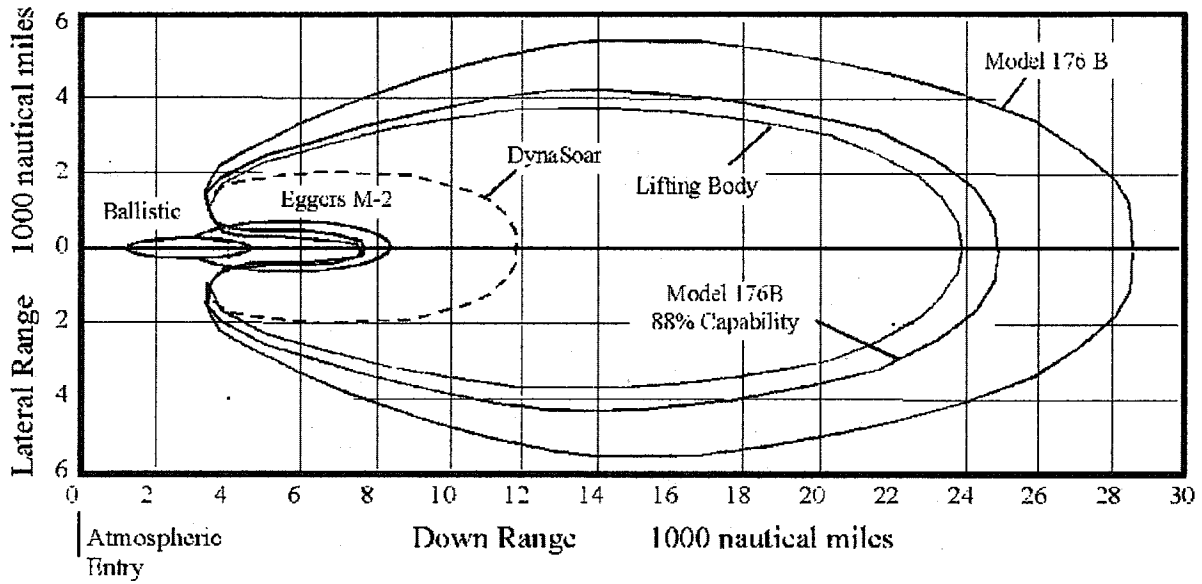


Figure 46. Landing Ellipses for (from left) Apollo Capsule, NASA Ames M2/F2, USAF X-20 DynaSoar, FDL Lifting-Body, 88%-Capability MDC Model 176H, and MDC 176H

The space shuttle landing ellipse would be inside the DynaSoar (X-20) ellipse, as its cross range is one missed orbit, or 1,555 nautical miles. The down range would be approximately 9,800 nautical miles. The ellipse is offset from 0,0 and has an indentation into some of the landing ellipse. This is an area the glider cannot reach with the aerodynamic and structural limits. The ballistic example is for the Apollo capsule, which had an L/D of about 0.5; Gemini and Mercury ellipses would be smaller. The Model 176B or Model 176H using 88 percent of its glide capability would have a glide range equal to the Earth's equatorial circumference.

- ¹ Bruno, Claudio & Czysz, Paul, "Future Spacecraft Propulsion Systems," Second Edition, Springer In conjunction with Praxis Publishing, Chichester, UK, 20089.
- ² Neyland, V. Ya., Scientific and Engineering Problems and Methods of Preflight Development of Orbiters, Draft Original of TsAGI paper, 1990.
- ³ Private Communication with Vladimir Plolith, AIAA Aerospace Sciences Conference, 1991.
- ⁴ DuPont, Anthony A., "Further Studies of Optimized Inlets for Hypersonic Turbine Engines," ISABE 99-7039, 14th International Symposium for Air Breathing Engines (ISABE), Florence, Italy, September 1999.
- ⁵ Buck, M.L., Zima, W.P., Kirkham, F.S. & Jones, R.A., "Joint USAF/NASA Hypersonic Research Aircraft Study," AIAA 75-1039, AIAA 25th Aircraft Systems and Technology Meeting, Los Angeles, California, August 1975.
- ⁶ Küchemann, D., "The Aerodynamic Design of Aircraft - A Detailed Introduction to the Current Aerodynamic Knowledge and Practical Guide to the Solution of Aircraft Design Problems," First Edition, Pergamon Press, 1978.
- ⁷ Draper, Alfred C., Buck, Melvin L., Goesch, William H., "A Delta Shuttle Orbiter," *Astronautics & Aeronautics*, Vol. 9, No 1, 26-36, Washington DC, January 1971.
- ⁸ *Astronautics & Aeronautics*, January 1971, Vol 9, No 1.
- ⁹ Dana, William, X-15, X24A, X24B pilot, Private Communications, 1973, 1998.
- ¹⁰ DuPont, Anthony A., "Further Studies of Optimized Inlets for Hypersonic Turbine Engines," ISABE 99-7039, 14th International Symposium for Air Breathing Engines (ISABE), Florence, Italy, September 1999.
- ¹¹ "Advanced Engine Development at Pratt & Whitney," SAE, 2001.
- ¹² Dawes, A. S. & Clarke, J.F., "Nonequilibrium Gas Flows in Entropy Layers," CoA Report No. NFP8802, College of Aeronautics, Cranfield Institute of Technology, Cranfield, 1988.
- ¹³ Glass, D., Camarada, C. et. al., "Fabrication and Testing of a Leading-Edge-Shaped Heat Pipe," AIAA-99-4866, 9th International Space Planes and Hypersonic Systems and Technologies Conference, Norfolk, Va. Nov. 1999.
- ¹⁴ Dick Mulready, "Advanced Engine Development at Pratt & Whitney" Society of Automotive Engineers.
- ¹⁵ Ahern, J.E., "Thermal Management of Air-Breathing Propulsion Systems," AIAA 92-0514, 30th Aerospace Sciences Meeting, Reno, Nevada, January 1992.
- ¹⁶ Maurice, L.Q., Leingang, J.L., & Carreiro, L.R., "The Benefits of In-Flight LOX Collection for Air Breathing Space Boosters," AIAA paper, 4th International Aerospace Planes Conference, Orlando, Florida, December 1992.
- ¹⁷ Rudakov, A.S. & Balepin, V.V., "Propulsion Systems with Air Pre-cooling for Aerospaceplanes," SAE 911183, SAE Aerospace Atlantic, April 1991, Dayton, Ohio.
- ¹⁸ Rudakov A.S., Gatin R.Y., Dulepov N.P., Korolnik B.N., Harchevnikova G.D & Yugov O.K.; "Analysis of Efficiency of Systems with Oxidizer Liquefaction and Accumulation for Improvement of Spaceplane Performance": IAF-91-270: 42nd Congress of the International Astronautical Federation : Montreal October 1991.
- ¹⁹ Balepin, V.V., Harchermikova, G.D., Tjurikov, E.V., & Avramenko, A.Ju., "Flight Liquid Oxygen Plants for Aerospace Plane: Thermodynamic and Integration Aspects," SAE chapter, 1993 SAE Aerospace Atlantic Conference and Exposition, Dayton, Ohio, April 1993.
- ²⁰ Aoki, T., Ito, T., et.al., "A Concept of LACE for SSTO Space Plane," AIAA-91-5011, AIAA 3rd International Aerospace Planes Conference, Orlando, Florida, December 1991.
- ²¹ Miki, Y., Taguchi, H., & Aoki, H., "Status and Future Planning of LACE Development," AIAA-93-5124, 5th International Aerospace Planes & Hypersonic Technology Conference, November 1993, Munich, Germany.
- ²² Anon., "Hyperplane," 39th International Astronautical Federation Congress, Bangalore India, October 1988.
- ²³ Anon., "An-2254/Interim HoToL Launch System Study," Presented to the European Space Agency in Paris, 21 June 1991. Representing the participants, Antonov DB, Bae (Space Systems), Chemical Automatics DB, NPO Molnyia, TsAGI and TsAM.
- ²⁴ Dick Mulready, "Advanced Engine Development at Pratt & Whitney" Society of Automotive Engineers.
- ²⁵ P. Hendrick and M Saint-Mard, "KLIN Blended Lifting Body VTOHL S.S.T.O., Trajectory and Sizing Calculations" Ecole Royale Militaire, Brussels Belgium, March 1998.
- ²⁶ DuPont, Anthony A., "Further Studies of Optimized Inlets for Hypersonic Turbine Engines," ISABE 99-7039, 14th International Symposium for Air Breathing Engines (ISABE), Florence, Italy, September 1999.
- ²⁷ Czysz, Paul A., "Evaluation and Analysis of the New Rocket-Based Combined Cycle For Reusable Launch Vehicles," HTC-9901, for MSE Technology Applications, Inc. 30 Nov 1999.
- ²⁸ Crutchner, Harold L., "Selected Meridional Cross Sections of Heights, Temperatures and Dew Points of the Northern Hemisphere," NAVAIR-50-1C-59, Published by Direction of the Commander, Naval Weather Service Command, 1965.
- ²⁹ *Astronautics & Aeronautics*, January 1971, Vol 9, No 1, Figure 3-11.
- ³⁰ Draper, Alfred C., Buck, Melvin L., Goesch, William H., "A Delta Shuttle Orbiter," *Astronautics & Aeronautics*, Vol. 9, No 1, 26-36, Washington DC, January 1971.
- ³¹ Anon., "Hypersonic Research Facilities Study, Volumes I through VI," NASA CR 114322 through 114331, Contract NAS2-5458, OART, NASA October 1970, declassified 1972.
- ³² Gaubatz, William A., "Space Transportation Infrastructure for Opening the Space Frontier-An International effort," The International Workshop on Space Plane/ RLV Technology Demonstrators, Tokyo, Japan, March 1997.
- ³³ Koelle, H.H. "Space Power" IAF-93-IAF Congress, Norway.
- ³⁴ Anon., "Hypersonic Research Facilities Study, Volumes I through VI," NASA CR 114322 through 114331, Contract NAS2-5458, OART, NASA October 1970, declassified 1972.